AD-A106 544 OHIO STATE UNIV COLUMBUS ELECTROSCIENCE LAB F/G 20/14
A STUDY OF EIGENVALUE BEHAVIOR IN ADAPTIVE ARRAYS.(U)
AUG 81 K SUEN
UNCLASSIFIED ESL-713603-2 N00019-81-C-0093
NL

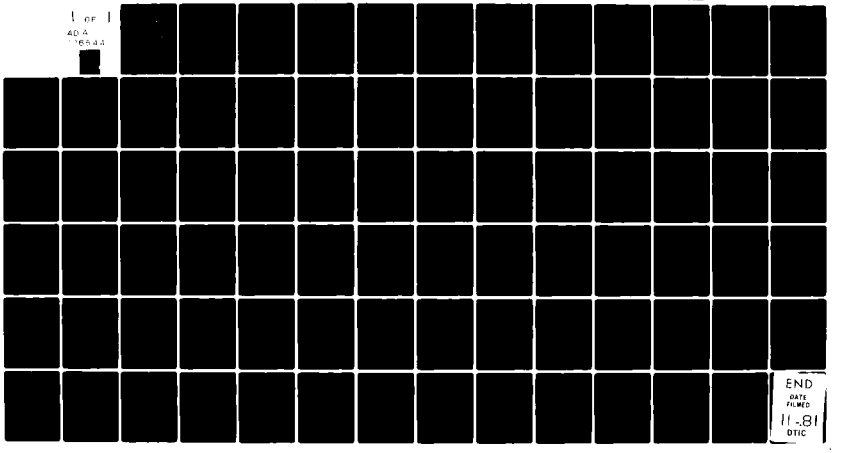

OSU

The Ohio State University

A STUDY OF EIGENVALUE BEHAVIOR IN ADAPTIVE ARRAYS

Kah-jing Suen

12

LEVEL II

The Ohio State University

ElectroScience Laboratory

Department of Electrical Engineering
Columbus, Ohio 43212

Technical Report 713603-2

August 1981

Contract No. N00019-81-C-0093

Naval Air Systems Command
Washington, D.C. 20361

NOTICES

When Government drawings, specifications, or other data are used for any purpose other than in connection with a definitely related Government procurement operation, the United States Government thereby incurs no responsibility nor any obligation whatsoever, and the fact that the Government may have formulated, furnished, or in any way supplied the said drawings, specifications, or other data, is not to be regarded by implication or otherwise as in any manner licensing the holder or any other person or corporation, or conveying any rights or permission to manufacture, use, or sell any patented invention that may in any way be related thereto.

UNCLASSIFIED

SECURITY CLASSIFICATION OF THIS PAGE *(When Data Entered)*

REPORT DOCUMENTATION PAGE		READ INSTRUCTIONS BEFORE COMPLETING FORM
1. REPORT NUMBER	2. GOVT ACCESSION NO. AD A106 544	3. RECIPIENT'S CATALOG NUMBER
4. TITLE *(and Subtitle)* A STUDY OF EIGENVALUE BEHAVIOR IN ADAPTIVE ARRAYS		5. TYPE OF REPORT & PERIOD COVERED Technical Report
		6. PERFORMING ORG. REPORT NUMBER ESL-713603-2
7. AUTHOR(s) Kah-jing/Suen		8. CONTRACT OR GRANT NUMBER(s) N00019-81-C-0093
9. PERFORMING ORGANIZATION NAME AND ADDRESS The Ohio State University, ElectroScience Laboratory, Department of Electrical Engineering, Columbus, Ohio 43212		10. PROGRAM ELEMENT, PROJECT, TASK AREA & WORK UNIT NUMBERS
11. CONTROLLING OFFICE NAME AND ADDRESS Naval Air Systems Command Washington, D.C. 20361		12. REPORT DATE August 1981
		13. NUMBER OF PAGES 79
14. MONITORING AGENCY NAME & ADDRESS *(if different from Controlling Office)*		15. SECURITY CLASS. *(of this report)*
		15a. DECLASSIFICATION/DOWNGRADING SCHEDULE

16. DISTRIBUTION STATEMENT *(of this Report)*

APPROVED FOR PUBLIC RELEASE:
DISTRIBUTION UNLIMITED

17. DISTRIBUTION STATEMENT *(of the abstract entered in Block 20, if different from Report)*

18. SUPPLEMENTARY NOTES

The work reported in this report was also used as a thesis submitted to the Department of Electrical Engineering, The Ohio State University as partial fulfillment for the degree Master of Science.

19. KEY WORDS *(Continue on reverse side if necessary and identify by block number)*

Adaptive Arrays
Eigenvalues

20. ABSTRACT *(Continue on reverse side if necessary and identify by block number)*

This report discusses the eigenvalues of the covariance matrix for an N-element LMS adaptive array. The effects of the signal and array parameters on these eigenvalues are discussed. A simple relation between the array output SINR and one of the eigenvalues is obtained for the case of strong interference and CW signals.

DD FORM 1 JAN 73 1473 EDITION OF 1 NOV 65 IS OBSOLETE

UNCLASSIFIED

SECURITY CLASSIFICATION OF THIS PAGE *(When Data Entered)*

TABLE OF CONTENTS

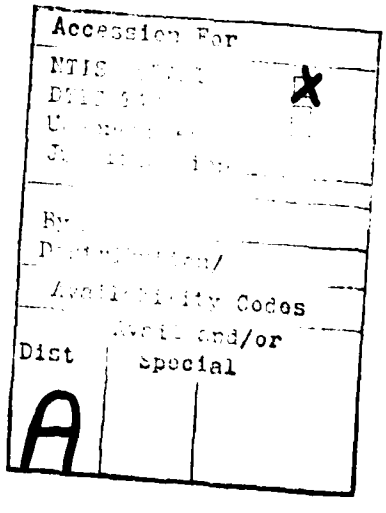

CHAPTER I
INTRODUCTION

Adaptive arrays have been under study in recent years as a means of protecting radar and communication systems from interference. These arrays are based on the original work of Applebaum and Widrow et al. Applebaum[1] presented an array control loop that maximizes a generalized signal-to-noise ratio (SNR). Widrow and his co-workers[2] presented the least mean square (LMS) error algorithm, based upon the method of steepest descent. Both the Applebaum array and the LMS array have found extensive applications in radar and communication systems.

One of the problems in applying adaptive arrays to communication systems is that the array speed of response varies with signal strengths. The array speed of response is determined by the eigenvalues of the so-called covariance matrix, which is the matrix of the cross products between the array element signals. These eigenvalues depend on signal powers. A strong signal produces a large eigenvalue and a weak signal produces a small eigenvalue. If, for example, the array must null interference 40 dB above thermal noise, the largest eigenvalue will be approximately 10^4 times larger than the smallest one. It is important to keep the range of variation of the eigenvalues as small as possible.

The eigenvalues not only depend on signal strengths, they also depend on the signal arrival angles, the signal bandwidths, and the array parameters (element spacings and element patterns).

The purpose of this report is to investigate and characterize the actual behavior of the eigenvalues in some simple adaptive arrays.

We examine here arrays with up to four elements and determine the exact eigenvalue behavior as a function of signal strengths, bandwidths, angles of arrival and array parameters.

Although the problem of eigenvalue spread in adaptive arrays is well known, very little data exists in the literature showing actual eigenvalue behavior. Some information on eigenvalues has been given by Gabriel[3], who discusses this subject in connection with retrodirective eigenvector beams. His paper also gives some qualitative descriptions of the effects of eigenvalues on array performance. Mayhan[4] has also presented some data on eigenvalues for multiple beam antennas. He has considered the eigenvalues for non-zero bandwidth signals by regarding the bandwidth as a perturbation of the original CW covariance matrix[5]. However, these papers do not give a complete overview of eigenvalue behavior as a function of the signal and array parameters. Our purpose here is to provide such data for some simple arrays.

We begin in Chapter II by establishing notation and formulating the problem. We then derive the eigenvalues for the case of two incoming signals, one desired and one interference. To simplify the problem, we first work out the solution for zero-bandwidth (CW) signals. In Chapter II-C, we develop an interesting relation between the array output signal-to-interference-plus-noise ratio (SINR) and the eigenvalues. We show that when the interference is very strong, the array output SINR is equal to one of the eigenvalues less one. Chapter III presents numerical results illustrating the effects of signal parameters (strengths, arrival angles and bandwidths) and array parameters (number of elements, element spacings and patterns) on eigenvalue behavior. Chapter IV contains the conclusions.

CHAPTER II
FORMULATION OF THE PROBLEM

A. Definition and Notation

Consider an N-element adaptive array as shown in Figure 1. The N elements are assumed to lie along a straight line with spacing D_ℓ between the ℓ^{th} element and the first element. The analytic signal $\tilde{x}_\ell(t)$ from the ℓ^{th} element is multiplied by a complex weight $w_\ell(t)$ generated from the optimizing network. The resultant products are summed to produce the array output signal $\tilde{s}(t)$. For an LMS array, the weight vector

$$W = [w_1, w_2 \cdots w_N]^T \tag{1}$$

satisfies the first order differential equation

$$\frac{dW}{dt} + k\Phi W = kS \tag{2}$$

where Φ is the covariance matrix of the array,

$$\Phi = E\{X^* X^T\} \tag{3}$$

S is the reference correlation vector,

$$S = E\{X^* \tilde{r}(t)\} \tag{4}$$

and k the loop gain. In these equations, X is the signal vector

$$X = [\tilde{x}_1(t), \tilde{x}_2(t), \cdots, \tilde{x}_N(t)]^T \tag{5}$$

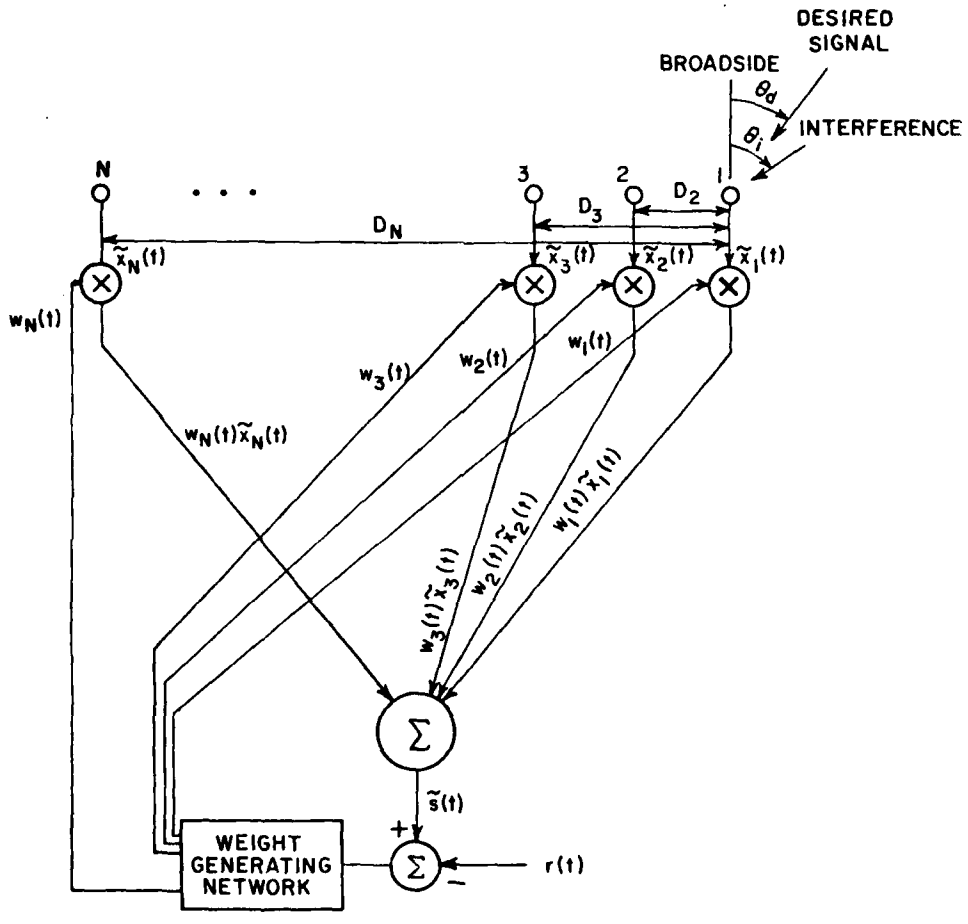

Figure 1. An N-element adaptive array with two incoming signals.

$\tilde{r}(t)$ is the (complex) reference signal in the array, T denotes transpose, * complex conjugate and $E\{\cdot\}$ expectation.

As will be seen below, Φ is not singular as long as the element signals contain independent thermal noise. Therefore, the inverse of Φ is always well defined. Let this inverse be denoted by Φ^{-1}, and then from Equation (2) the steady-state weight vector is

$$W_{st} = \Phi^{-1}S \tag{6}$$

where the subscript "st" denotes steady-state. The complete time response of the weight vector is then

$$W(t) = \sum_{\ell=1}^{M} C_{\ell} e^{-k\lambda_{\ell}t} + \Phi^{-1}S \tag{7}$$

where the C_{ℓ}'s are constant vectors depending on the initial conditions of the weights at t=0. The λ_{ℓ}'s are the distinct eigenvalues of Φ and M is the number of distinct eigenvalues. It is these eigenvalues that control the transient response of the array weights and that concern us in this report.

We shall determine the eigenvalues of Φ under the condition that there are two signals coming into the array. One is the desired signal arriving from angle θ_d and the other interference from θ_i. Both angles are measured with respect to broadside, as shown in Figure 1. We also assume each element signal contains a thermal noise component. Thus, the analytic signal behind the ℓ^{th} element is written

$$\tilde{x}_{\ell}(t) = \tilde{d}_{\ell}(t) + \tilde{i}_{\ell}(t) + \tilde{n}_{\ell}(t) \tag{8}$$

where $\tilde{d}_{\ell}(t)$ and $\tilde{i}_{\ell}(t)$ are the received desired signal and interference on the ℓ^{th} element, respectively, and $\tilde{n}_{\ell}(t)$ is the element noise.

The above equation suggests that we can divide the signal vector X into the sum of three component vectors, i.e.,

$$X = X_d + X_i + X_n \tag{9}$$

with

$$X_d = [\tilde{d}_1(t), \tilde{d}_2(t), \cdots, \tilde{d}_N(t)]^T \tag{10}$$

the desired signal vector,

$$X_i = [\tilde{i}_1(t), \tilde{i}_2(t), \cdots, \tilde{i}_N(t)]^T \tag{11}$$

the interference vector, and

$$X_n = [\tilde{n}_1(t), \tilde{n}_2(t), \cdots, \tilde{n}_N(t)]^T \tag{12}$$

the noise vector.

We shall assume here that the desired signal, the interference and the noises are zero mean Gaussian random processes uncorrelated with each other. Thus, the signal vectors are statistically independent of each other, i.e.,

$$E\{X_d^* X_i^T\} = E\{X_d^* X_n^T\} = E\{X_i^* X_d^T\} = E\{X_i^* X_n^T\} = E\{X_n^* X_d^T\}$$

$$= E\{X_n^* X_i^T\} = 0 \ .$$

Then from Equations (3) and (9), we have

$$\Phi = E\{(X_d+X_i+X_n)^*(X_d+X_i+X_n)^T\} \tag{13}$$

$$= E\{X_d^* X_d^T\} + E\{X_i^* X_i^T\} + E\{X_n^* X_n^T\} \tag{14}$$

$$= \Phi_d + \Phi_i + \Phi_n \ . \tag{15}$$

Consider first the desired signal. It is clear from Equation (15) that the desired signal part of the covariance matrix, Φ_d, is

$$\Phi_d = E\{X_d^* X_d^T\} = [\Phi_{d_{\ell m}}] \tag{16}$$

where $\Phi_{d_{\ell m}}$ denotes the matrix element of Φ_d at the ℓ^{th} row and the m^{th} column. From Equations (10) and (16), we know that

$$\Phi_{d_{\ell m}} = E\{\tilde{d}_\ell^*(t)\tilde{d}_m(t)\} \quad . \tag{17}$$

Because of the interelement propagation delays, we can write

$$\tilde{d}_\ell(t) = f_\ell(\theta_d)\tilde{d}(t-T_{d_\ell}) \tag{18}$$

where T_{d_ℓ} denotes the interelement time delay between element ℓ and element 1, $\tilde{d}(t)$ is the desired signal waveform and $f_\ell(\theta)$ is the voltage response of the ℓ^{th} element to a unit amplitude test signal arriving from angle θ. In Equation (18) we have assumed that the element patterns are independent of the signal frequencies over the bandwidth of the desired signal $\tilde{d}(t)$. Thus from Equations (17) and (18), we have

$$\Phi_{d_{\ell m}} = f_\ell^*(\theta_d)f_m(\theta_d)E\{\tilde{d}^*(t-T_{d_\ell})\tilde{d}(t-T_{d_m})\} \tag{19}$$

The time delays in the above equations are determined by the element spacings and the signal arrival angles, i.e.,

$$T_{d_\ell} = \frac{D_\ell}{c} \sin\theta_d \tag{20}$$

with c the velocity of propagation.

In order to evaluate the expectation in Equation (19), we use the following definition. Let the desired signal be a stationary random process with autocorrelation function

$$R_{\tilde{d}}(\tau) = E\{\tilde{d}^*(t)\tilde{d}(t+\tau)\} \tag{21}$$

$$= E\{\tilde{d}^*(t-\tau)\tilde{d}(t)\} \quad . \tag{22}$$

Then we can rewrite Equation (19) as

$$\Phi_{d_{\ell m}} = f_\ell^*(\theta_d) f_m(\theta_d) R_{\tilde{d}}(T_{d_\ell} - T_{d_m}) \tag{23}$$

Furthermore, we assume that the desired signal has a flat, band-limited power spectral density $S_{\tilde{d}}(\omega)$ centered at ω_o as shown in Figure 2. Within the band $\Delta\omega_d$ the desired signal has power density $2\pi P_d/(\Delta\omega_d)$, with P_d the desired signal power. Then the autocorrelation function is given by

$$R_{\tilde{d}}(\tau) = \frac{1}{2\pi} \int_{-\infty}^{\infty} S_{\tilde{d}}(\omega) e^{j\omega\tau} \, d\omega \tag{24}$$

$$= P_d \frac{\sin \frac{\Delta\omega_d \tau}{2}}{\frac{\Delta\omega_d \tau}{2}} e^{j\omega_o \tau} \quad . \tag{25}$$

Combining Equations (23) and (25), we have

$$\Phi_{d_{\ell m}} = f_\ell^*(\theta_d) f_m(\theta_d) P_d \, \mathrm{sinc}\left[\frac{1}{2} \Delta\omega_d (T_{d_\ell} - T_{d_m})\right] e^{j\omega_o (T_{d_\ell} - T_{d_m})} \tag{26}$$

with $\mathrm{sinc}\, x = \frac{\sin x}{x}$.

We can simplify the above result by noting that $\omega_o T_{d_\ell}$ is just the phase shift between element 1 and element ℓ at the center frequency ω_o. Let us define this phase shift to be

$$\Phi_{d_\ell} = \omega_o T_{d_\ell} \quad . \tag{27}$$

Upon substitution of Equation (20) into Equation (27), we get

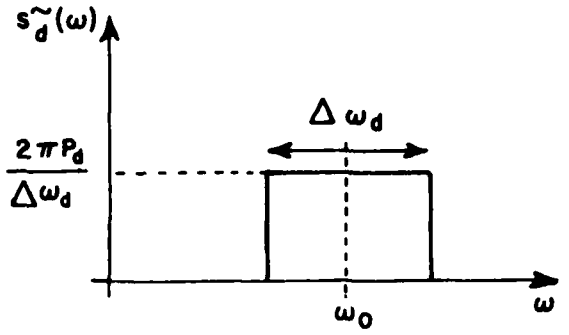

Figure 2. Power spectral density of the desired signal, $S_{\tilde{d}}(\omega)$.

$$\phi_{d_\ell} = \frac{2\pi D_\ell}{\lambda_o} \sin\theta_d \tag{28}$$

with λ_o the wavelength at the center frequency ω_o. In addition,

$$\frac{\Delta\omega_d T_{d_\ell}}{2} = \frac{1}{2}\left(\frac{\Delta\omega_d}{\omega_o}\right)\left(\omega_o T_{d_\ell}\right) = \frac{1}{2} B_d \phi_{d_\ell} \tag{29}$$

where

$$B_d = \frac{\Delta\omega_d}{\omega_o} \tag{30}$$

is the fractional bandwidth of the desired signal.

Substituting Equation (29) into Equation (26), we finally have

$$\Phi_{d_{\ell m}} = f_\ell^*(\theta_d) f_m(\theta_d) P_d \operatorname{sinc}\left[\frac{1}{2} B_d(\phi_{d_\ell} - \phi_{d_m})\right] e^{j(\phi_{d_\ell} - \phi_{d_m})} . \tag{31}$$

Similar results may be derived for the interference. We have

$$\tilde{i}_\ell(t) = f_\ell(\theta_i)\tilde{i}(t - T_{i_\ell}) \tag{32}$$

where $\tilde{i}(t)$ is the interference waveform and

$$T_{i_\ell} = \frac{D_\ell}{c} \sin\theta_i \quad . \tag{33}$$

From the previous discussion, we know that the ℓm^{th} element of the interference part of the covariance matrix, Φ_i, is given by

$$\Phi_{i_{\ell m}} = f_\ell^*(\theta_i) f_m(\theta_i) E\{\tilde{i}^*(t-T_{i_\ell})\tilde{i}(t-T_{i_m})\} \quad . \tag{34}$$

We define the autocorrelation function of the interference as

$$R_{\tilde{i}}(\tau) = E\{\tilde{i}^*(t)\tilde{i}(t+\tau)\} \tag{35}$$

$$= E\{\tilde{i}^*(t-\tau)\tilde{i}(t)\} \tag{36}$$

$$= P_i \operatorname{sinc}\left[\frac{1}{2} \Delta\omega_i \tau\right] e^{j\omega_o \tau} \tag{37}$$

where we have assumed the interference also has a flat, band-limited power spectral density of bandwidth $\Delta\omega_i$, as shown in Figure 3. Hence, Equation (34) becomes

$$\Phi_{i_{\ell m}} = f_\ell^*(\theta_i) f_m(\theta_i) P_i \operatorname{sinc}\left[\frac{1}{2} B_i(\phi_{i_\ell} - \phi_{i_m})\right] e^{j(\phi_{i_\ell} - \phi_{i_m})} \quad . \tag{38}$$

where

$$B_i = \frac{\Delta\omega_i}{\omega_o} \tag{39}$$

is the fractional bandwidth of the interference and

$$\phi_{i_\ell} = \frac{2\pi D_\ell}{\lambda_o} \sin\theta_i \tag{40}$$

is the interelement phase shift between the ℓ^{th} element and the first element for the interference.

Finally, we assume the noises are zero mean Gaussian random processes uncorrelated with each other, each with power σ^2. Thus,

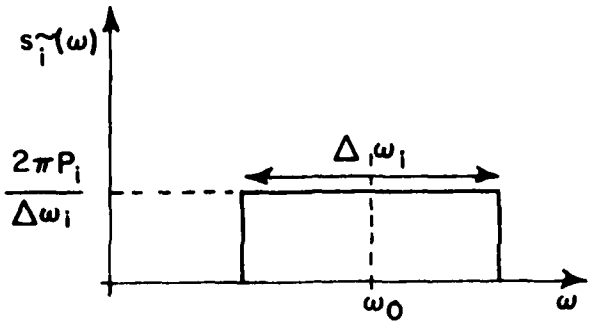

Figure 3. Power spectral density of the interference, $S_{\tilde{i}}(\omega)$.

$$E\{\tilde{n}_\ell^*(t)\tilde{n}_m(t)\} = \sigma^2\delta_{\ell m} \tag{41}$$

with $\delta_{\ell m}$ the Kronecker delta function. Therefore, the noise part of the covariance matrix is

$$\Phi_n = \sigma^2 I \tag{42}$$

with I denoting the identity matrix.

From Equations (15), (31), (38) and (42) we conclude that the ℓm^{th} element of Φ is

$$\begin{aligned}\Phi_{\ell m} = {} & f_\ell^*(\theta_d)f_m(\theta_d)P_d \ \text{sinc}\left[\frac{1}{2}B_d(\phi_{d_\ell}-\phi_{d_m})\right] e^{j(\phi_{d_\ell}-\phi_{d_m})} \\ & + f_\ell^*(\theta_i)f_m(\theta_i)P_i \ \text{sinc}\left[\frac{1}{2}B_i(\phi_{i_\ell}-\phi_{i_m})\right] e^{j(\phi_{i_\ell}-\phi_{i_m})} \\ & + \sigma^2\delta_{\ell m} \quad .\end{aligned} \tag{43}$$

In a later section of this report, we shall investigate the eigenvalues of Φ for arbitrary bandwidths. First, however, we shall

consider the special case of zero bandwidth (CW) signals because in this case we can obtain the eigenvalues in simple analytical form.

B. Eigenvalues for Zero Bandwidth Signals

For $B_d=B_i=0$, the sinc function in Equation (43) is unity, so Equation (43) simplifies to

$$\Phi_{\substack{\ell m \\ cw}} = P_d f_\ell^*(\theta_d) f_m(\theta_d) e^{j(\phi_{d_\ell} - \phi_{d_m})} + P_i f_\ell^*(\theta_i) f_m(\theta^i) e^{j(\phi_{i_\ell} - \phi_{i_m})} + \sigma^2 \delta_{\ell m} \quad . \tag{44}$$

This result is equivalent to the form

$$\Phi_{cw} = P_d U_d^* U_d^T + P_i U_i^* U_i^T + \sigma^2 I \tag{45}$$

where

$$U_d = \left[f_1(\theta_d) e^{-j\phi_{d_1}}, f_2(\theta_d) e^{-j\phi_{d_2}}, \cdots, f_N(\theta_d) e^{-j\phi_{d_N}} \right]^T \tag{46}$$

and

$$U_i = \left[f_1(\theta_i) e^{-j\phi_{i_1}}, f_2(\theta_i) e^{-j\phi_{i_2}}, \cdots, f_N(\theta_i) e^{-j\phi_{i_N}} \right]^T \tag{47}$$

are vectors that contain the element patterns and interelement phases.

It is helpful to work with dimensionless quantities, and specifically to normalize the covariance matrix with respect to the noise power σ^2. We define

$$\Phi'_{cw} = \frac{\Phi_{cw}}{\sigma^2} = P_d U_d^* U_d^T + P_i U_i^* U_i^T + I \tag{48}$$

where

$$\xi_d = \frac{P_d}{\sigma^2}$$

= the signal-to-noise ratio (SNR) of the desired signal

and

$$\xi_i = \frac{P_i}{\sigma^2}$$

= the interference-to-noise ratio (INR) of the interference.

We shall determine the eigenvalues of Φ'_{cw} rather than Φ_{cw}. The eigenvalues of Φ_{cw} are equal to those of Φ'_{cw} times σ^2.

Because of the form of the covariance matrix in Equation (48), it is clear that two of the eigenvectors of Φ'_{cw} will lie in the plane formed by U_d^* and U_i^*. Hence we may express two eigenvectors (e) in the form

$$e = \alpha U_d^* + \beta U_i^* \tag{49}$$

where α and β are constants to be determined by the requirement

$$\Phi'_{cw} e = \lambda e \tag{50}$$

and λ is the corresponding eigenvalue. We may find α and β by substituting Equation (49) into Equation (50). Straightforward calculations show that

$$\Phi'_{cw}(\alpha U_d^* + \beta U_i^*) = (\alpha U_d^* + \beta U_i^*) + \alpha U_d^* \left(\xi_d U_d^T U_d^* + \frac{\beta}{\alpha} \xi_d U_d^T U_i^* \right) + \beta U_i^* \left(\xi_i U_i^T U_i^* + \frac{\alpha}{\beta} \xi_i U_i^T U_d^* \right) . \tag{51}$$

Hence Equation (49) will be a legitimate eigenvector if we choose α and β so that

$$\varepsilon_d U_d^T U_d^* + \frac{\beta}{\alpha}\varepsilon_d U_d^T U_i^* = \varepsilon_i U_i^T U_i^* + \frac{\alpha}{\beta}\varepsilon_i U_i^T U_d^* \quad . \tag{52}$$

Therefore, from Equations (50), (51) and (52), we have

$$\lambda = 1 + \varepsilon_d U_d^T U_d^* + \frac{\beta}{\alpha}\varepsilon_d U_d^T U_i^* \quad , \tag{53}$$

or equivalently

$$\lambda = 1 + \varepsilon_i U_i^T U_i^* + \frac{\alpha}{\beta}\varepsilon_i U_i^T U_d^* \quad . \tag{54}$$

By defining

$$\frac{\beta}{\alpha} = Y \tag{55}$$

and then transforming Equation (42) into a quadratic equation, we get

$$Y^2\varepsilon_d U_d^T U_i^* - (\varepsilon_i U_i^T U_i^* - \varepsilon_d U_d^T U_d^*)Y - \varepsilon_i U_i^T U_d^* = 0 \quad . \tag{56}$$

This quadratic equation is readily solved to give two solutions,

$$Y_1 = \frac{1}{2\varepsilon_d U_d^T U_i^*}(a+b) \tag{57}$$

$$Y_2 = \frac{1}{2\varepsilon_d U_d^T U_i^*}(a-b) \tag{58}$$

where

$$a = \varepsilon_i U_i^T U_i^* - \varepsilon_d U_d^T U_d^* \tag{59}$$

and

$$b = (a^2 + 4\varepsilon_i\varepsilon_d |U_i^T U_d^*|^2)^{1/2} \quad . \tag{60}$$

According to Equation (53), we then have two eigenvalues,

$$\lambda_1 = 1 + \varepsilon_d U_d^T U_d^* + \frac{1}{2}(a+b) \tag{61}$$

$$\lambda_2 = 1 + \varepsilon_d U_d^T U_d^* + \frac{1}{2}(a-b) \tag{62}$$

Since we have an N element array, Φ'_{cw} is an N by N matrix so there are N eigenvalues. In addition to the above two, there are N-2 additional eigenvalues. To find these, we note that if e_1 is an arbitrary vector orthogonal to both U_d^* and U_i^*, then

$$\Phi'_{cw} e_1 = e_1 + \varepsilon_d U_d^* (U_d^T e_1) + \varepsilon_i U_i^* (U_i^T e_1) = e_1 \tag{63}$$

since $U_d^T e_1 = U_i^T e_1 = 0$ from the orthogonality. This result implies that e_1 is also an eigenvector of Φ'_{cw} with unity eigenvalue. In general, since Φ'_{cw} is of order N, we can find N-2 such vectors orthogonal to both U_d^* and U_i^*. Hence the remaining N-2 eigenvalues are all unity.

We now have found all N eigenvalues of Φ'_{cw}. In the following paragraphs, we shall make some observations about the results obtained.

First, all the eigenvalues of Φ'_{cw} are real because Φ'_{cw} is a Hermitian matrix. Moreover,

$$\lambda_\ell \geq 1 \tag{64}$$

for $\ell = 1, 2, \cdots, N$ since both $\varepsilon_d U_d^* U_d^T$ and $\varepsilon_i U_i^* U_i^T$ in Equation (48) are non-negative definite matrices. To see this, consider for example $\varepsilon_d U_d^* U_d^T$. It is easily seen that

$$\varepsilon_d (U_d^* U_d^T) U_d^* = (\varepsilon_d U_d^T U_d^*) U_d^* \tag{65}$$

where $\varepsilon_d U_d^T U_d^*$ is a non-negative quantity. Thus U_d^* is an eigenvector of $\varepsilon_d U_d^* U_d^T$ with eigenvalue $\varepsilon_d U_d^T U_d^* \geq 0$. For any other vector U^* perpendicular to U_d^*, we have

$$(U_d^* U_d^T) U^* = (U_d^T U^*) U_d^* = 0\ U_d^* \tag{66}$$

so U^* is also an eigenvector of $U_d^* U_d^T$ with zero eigenvalue. In N space, there will have N-1 vectors U^* perpendicular to U_d^* and to each other, and hence N-1 zero eigenvalues. Therefore $\varepsilon_d U_d^* U_d^T$ is of rank one and the only non-zero eigenvalue is $\varepsilon_d U_d^T U_d^*$. Thus $\varepsilon_d U_d^* U_d^T$ is non-negative definite. Likewise, $\varepsilon_i U_i^* U_i^T$ is also a non-negative definite matrix, so the sum

$$A = \varepsilon_d U_d^* U_d^T + \varepsilon_i U_i^* U_i^T \tag{67}$$

is non-negative definite. Since Φ'_{CW} in Equation (48) is the sum of the identity matrix and the non-negative definite matrix A in Equation (67), the eigenvalues of Φ'_{CW} are just the eigenvalues of A plus unity. Thus

$$\lambda(\Phi'_{CW}) = \lambda(I+A) = 1+\lambda(A) \geq 1 \tag{68}$$

where $\lambda(\cdot)$ denotes 'the eigenvalues of'.

Note that in general the number of eigenvalues of Φ'_{CW} different from unity is equal to the number of signals incident on the array. When the array receives no signals other than the thermal noise, the normalized covariance matrix of Eqution (48) is simply

$$\Phi'_{CW} = I \quad .$$

In this case, all the eigenvalues are unity. If one CW signal, characterized by strength ε and arrival angle θ, is incident on the array, then the covariance matrix becomes

$$\Phi'_{CW} = \varepsilon U^* U^T + I \tag{69}$$

In this case, one of the eigenvalues of Φ'_{CW} is $1+\varepsilon U^T U^*$ and the remaining N-1 are all unity. From the earlier discussion, it is clear that with two input signals there are two eigenvalues different from unity. In general, one may show that with K CW input signals (K<N) there are K non-unity eigenvalues and the remaining N-K eigenvalues are unity.*

Note that when only one signal is incident on the array, the one eigenvalue different from unity has a simple form. Using the definition of a typical signal vector as Equation (46), we see that

$$1 + \varepsilon U^T U^* = 1 + \varepsilon \sum_{\ell=1}^{N} |f_\ell(\theta)|^2 \quad . \tag{70}$$

Hence this eigenvalue is independent of the element spacings in the array but is a function of signal arrival angle θ. Moreover, if the element patterns are chosen so that

$$\sum_{\ell=1}^{N} |f_\ell(\theta)|^2$$

does not vary with θ (as, for example, with isotropic elements) then this eigenvalue is constant for all θ.

Next, we note that λ_1 and λ_2 in Equations (61) and (62) depend strongly on the signal powers. For example, suppose the interference power is much stronger than the desired signal power. I.e., we have

$$\varepsilon_i U_i^T U_i^* >> \varepsilon_d U_d^T U_d^* \tag{71}$$

and

---

*This statement assumes that all K incoming signals produce linearly independent signal vectors.

$$\varepsilon_i >> \varepsilon_d \quad , \tag{72}$$

then in Equations (59) and (60) we may approximate a and b by

$$a \doteq \varepsilon_i U_i^T U_i^* \tag{73}$$

and

$$b \doteq a \tag{74}$$

In Equation (74) we have neglected the term $4\varepsilon_i\varepsilon_d\left|U_i^T U_d^*\right|^2$ of Equation (60) because it is small compared to a, since

$$\frac{4\varepsilon_i\varepsilon_d\left|U_i^T U_d^*\right|^2}{a^2} \doteq \frac{4\varepsilon_d}{\varepsilon_i}\frac{\left|U_i^T U_d^*\right|^2}{\left|U_i^T U_i^*\right|^2} \leq \frac{4\varepsilon_d}{\varepsilon_i} \doteq 0 \quad .$$

Therefore the two eigenvalues in Equations (61) and (62) can be written approximately as follows:

$$\lambda_1 = \varepsilon_i U_i^T U_i^* + 1 \tag{75}$$

$$\lambda_2 = \varepsilon_d U_d^T U_d^* + 1 \quad . \tag{76}$$

The above two formulas for the eigenvalues depend solely on signal arrival angles; the element spacings have no effect. It is clear that the largest eigenvalue λ_1 is essentially controlled by the large interference and the smaller eigenvalue λ_2 is controlled by the weaker desired signal. All other eigenvalues are unity with no dependence on the signal arrival angles.

Better approximations for the eigenvalues λ_1 and λ_2 may be obtained by using the binomial expansion to approximate b in Equation (60). That is, we use

$$(1+x)^{1/2} = 1 + \frac{1}{2}x$$

to get

$$b \cong a\left(1 + \frac{2\xi_i\xi_d}{a^2}\left|U_i^T U_d^*\right|^2\right) \quad . \tag{77}$$

Then putting Equation (77) into Equations (61) and (62), we get

$$\lambda_1 \cong 1 + \varepsilon_i U_i^T U_i^* + \frac{\xi_i\xi_d}{a}\left|U_i^T U_d^*\right|^2 \tag{78}$$

$$\lambda_2 \cong 1 + \varepsilon_d U_d^T U_d^* - \frac{\xi_i\xi_d}{a}\left|U_i^T U_d^*\right|^2 \tag{79}$$

The above approximations are more accurate than Equations (75) and (76).

We now consider the eigenvalues under two special conditions for $\left|U_i^T U_d^*\right|$. The first case is when the two signal vectors are parallel, i.e., when

$$U_i^* = h\, U_d^* \tag{80}$$

with h a complex constant. Clearly, under Equation (80) we have from Equations (59) and (60) that

$$a_{\|} = [|h|^2\varepsilon_i - \varepsilon_d]U_d^T U_d^* \tag{81}$$

and

$$b_{\|} = [a_{\|}^2 + 4|h|^2\varepsilon_i\varepsilon_d(U_d^T U_d^*)^2]^{1/2} \quad . \tag{82}$$

Hence we have

$$\lambda_{1_{\parallel}} = 1+\varepsilon_d U_d^T U_d^* + |h|^2 \varepsilon_i U_d^T U_d^* = 1+\varepsilon_d U_d^T U_d^* + \varepsilon_i U_i^T U_i^* \tag{83}$$

and

$$\lambda_{2_{\parallel}} = 1 \quad . \tag{84}$$

In the above equations, the subscript '$\parallel$' indicates that $a_{\parallel}$, $b_{\parallel}$, $\lambda_{1_{\parallel}}$ and $\lambda_{2_{\parallel}}$ are calculated under condition Equation (80). From our earlier result in Equation (64) it is clear that $\lambda_{2_{\parallel}}$ is the smallest possible value of λ_2.

On the other hand, if we have orthogonal signal vectors, i.e.,

$$\left| U_i^T U_d^* \right| = 0 \tag{85}$$

then from Equations (60), (61) and (62) we get

$$b_{\perp} = a_{\perp} \tag{86}$$

$$\lambda_{1_{\perp}} = 1 + \varepsilon_i U_i^T U_i^* \tag{87}$$

$$\lambda_{2_{\perp}} = 1 + \varepsilon_d U_d^T U_d^* \tag{88}$$

where the subscript '$\perp$' indicates that these quantities are obtained under condition Equation (85).

These special case eigenvalues specify the bounds within which the eigenvalues will vary with signal angles. To show this, we make the following observations. From Equation (60), it is clear that*

$$b > a \tag{89}$$

*Here, we assume that $a > 0$, i.e., $\varepsilon_i U_i^T U_i^* > \varepsilon_d U_d^T U_d^*$. The case for $a < 0$ can be similarly deduced.

Therefore, from Equation (62) we see that

$$\lambda_2 \leq 1 + \varepsilon_d U_d^T U_d^* \tag{90}$$

Combining with Equations (68), (84) and (88), we see clearly that

$$\lambda_{2_{\parallel}} \leq \lambda_2 \leq \lambda_{2_{\perp}} \quad . \tag{91}$$

This inequality gives the bounds within which λ_2 varies as a function of θ_d and θ_i. To get the corresponding bounds on λ_1 we proceed as follows. Rewrite Equation (61)

$$\lambda_1 = 1+\varepsilon_i U_i^T U_i^* + \frac{1}{2}(b-a) \quad . \tag{92}$$

Thus it is clear that

$$\lambda_1 \geq 1+\varepsilon_i U_i^T U_i^* \tag{93}$$

which gives a lower bound for λ_1. Making use of the Schwartz inequality

$$\left|U_i^T U_d^*\right|^2 \leq (U_i^T U_i^*)(U_d^T U_d^*) \quad , \tag{94}$$

we have from Equations (60) and (94) that

$$\begin{aligned} b^2 &= a^2+4\varepsilon_i\varepsilon_d\left|U_i^T U_d^*\right|^2 \\ &\leq a^2+4\varepsilon_i\varepsilon_d(U_i^T U_i^*)(U_d^T U_d^*) \\ &= (\varepsilon_i U_i^T U_i^*+\varepsilon_d U_d^T U_d^*)^2 \end{aligned} \tag{95}$$

i.e.,

$$b \leq \varepsilon_i U_i^T U_i^*+\varepsilon_d U_d^T U_d^* \quad . \tag{95}$$

Equation (61) can again be rewritten as

$$\lambda_1 = 1+\varepsilon_i U_i^T U_i^* + \varepsilon_d U_d^T U_d^* + \frac{1}{2}\left(b-\varepsilon_i U_i^T U_i^* - \varepsilon_d U_d^T U_d^*\right) \quad . \tag{96}$$

Therefore, from Equations (95) and (96), it is clear that

$$\lambda_1 = 1+\varepsilon_i U_i^T U_i^* + \varepsilon_d U_d^T U_d^* \quad . \tag{97}$$

Combining Equations (93), (97) and the previous results of $\lambda_{1_{II}}$ and $\lambda_{1_\perp}$, we have

$$\lambda_{1_\perp} \leq \lambda_1 \leq \lambda_{1_{II}} \quad . \tag{98}$$

Notice that the eigenvalues do not necessarily attain these bounds as the signal angles vary. An eigenvalue, say λ_2, will often have a maximum λ_{2max} smaller than $\lambda_{2_\perp}$. These bounds are determined simply from the signal strengths and terms such as $U^T U^*$ which involve the element patterns $|f_\nu(\theta)|^2$ but not the element spacings. Typically it is found that when the element spacings are larger than half-wavelength the extrema of the eigenvalues coincide with the bounds for isotropic element arrays.

Next, we consider the case of isotropic elements. With $f_\nu(\theta)=1$; $\nu=1,2,\cdots,N$ we have then

$$U_d^T U_d^* = U_i^T U_i^* = N = \text{the number of elements in the array.}$$

Thus the eigenvalues in Equations (61) and (62) have a simpler form

$$\lambda_1 = 1+N\varepsilon_d + \frac{1}{2}(a+b) \tag{99}$$

$$\lambda_2 = 1+N\varepsilon_d + \frac{1}{2}(a-b) \tag{100}$$

where

$$a = N(\varepsilon_i - \varepsilon_d)$$

$$b = (a^2 + 4\varepsilon_i\varepsilon_d \left| U_i^T U_d^* \right|^2)^{1/2} \tag{101}$$

The bounds in Equations (91) and (98) also reduce to

$$1 + N\varepsilon_i \leq \lambda_1 \leq 1 + N(\varepsilon_i + \varepsilon_d) \quad , \tag{102}$$

and

$$1 \leq \lambda_2 \leq 1 + N\varepsilon_d \quad . \tag{103}$$

Now the bounds depend on the signal strengths ε_i and ε_d only. It is clear from Equation (102) that for very strong interference, such that $\varepsilon_i >> \varepsilon_d$ and $\varepsilon_i >> 1$ hold, the variation in λ_1 is very small compared to its magnitude.

Since for isotropic elements the sum of λ_1 and λ_2 equals a constant, $2+N(\varepsilon_i+\varepsilon_d)$, we know that when λ_2 attains its minimum λ_1 must be at its maximum, and vice versa. We shall show the explicit conditions under which the eigenvalues attain their extrema with respect to signal arrival angles. For example, let us differentiate Equation (100) with respect to θ_i (with θ_d fixed). The result is

$$\frac{\partial \lambda_2}{\partial \theta_i} = -\frac{1}{2}\frac{\partial b}{\partial \theta_i} = -\frac{\varepsilon_i\varepsilon_d}{b}\frac{\partial}{\partial \theta_i}\left| U_i^T U_d^* \right|^2$$

$$= -\frac{2\varepsilon_i\varepsilon_d}{b}\left| U_i^T U_d^* \right| \left[\frac{\partial}{\partial \theta_i}\left| U_i^T U_d^* \right| \right] \quad . \tag{104}$$

Thus the extrema of λ_2 (with respect to θ_i) occur when

$$\left| U_i^T U_d^* \right| = 0 \tag{105}$$

or when

$$\frac{\partial}{\partial\theta_i}\left|U_i^T U_d^*\right| = 0 \qquad (106)$$

We see, then, that the orthogonal condition in Equation (85) is also the condition for λ_2 to reach its extrema with respect to θ_i. On the other hand, the parallel signal vector condition in Equation (80) satisfies Equation (106) because

$$\frac{\partial}{\partial\theta_i}\left|U_i^T U_d^*\right| = |h|\,\frac{\partial}{\partial\theta_i}\left|U_d^T U_d^*\right| = 0 \quad .$$

Therefore Equation (80) also gives the condition for λ_2 to be extrema. These results indicate that the extrema of the eigenvalues coincide with the bounds given in Equations (91) and (98) for isotropic elements.

We now return to arbitrary element patterns and consider how the condition in Equation (80) can be met. From the definition of U_d^* and U_i^* in Equations (46) and (47), it may be seen that the condition in Equation (80) requires suitable (θ_d,θ_i) pairs that satisfy N simultaneous equations, i.e.,

$$h\, f_\ell(\theta_d)e^{j\phi_{d_\ell}} = f_\ell(\theta_i)e^{j\phi_{i_\ell}} \qquad (107)$$

for $\ell=1,2,\cdots,N$. One solution to this is of course $\theta_d=\theta_i$ with $h=1$. Whether other θ_d and θ_i exist for which Equation (107) is satisfied depends on the element spacings and patterns. Actually, Equation (107) is just the condition for a grating null[6]. If the array does not have grating nulls, Equation (107) will not be satisfied except for $\theta_i=\theta_d$, so that λ's will not attain the bounds in Equations (91) and (98).

For isotropic elements, Equation (107) reduces to

$$e^{j\phi_{d_\ell}} = e^{j\phi_{i_\ell}} \qquad (108)$$

with h=1. This equation is always satisfied for $\theta_i=\theta_d$ and the symmetry angle $\theta_i=\pi-\theta_d$ since the array in Figure 1 has all elements along a straight line.

Finally, we define the eigenvalue spread S to be the ratio between λ_1 and λ_2. Since both λ_1 and λ_2 are functions of θ_d and θ_i we have

$$s(\theta_d,\theta_i) = \frac{\lambda_1(\theta_d,\theta_i)}{\lambda_2(\theta_d,\theta_i)} \quad . \tag{109}$$

This spread is then bounded by S_{min} and S_{max}, i.e.,

$$S_{min} \leq S \leq S_{max} \tag{110}$$

where, from Equations (84), (85) and (89)

$$S_{min} = \frac{\lambda_{1_{\parallel}}}{\lambda_{2_{\perp}}} = \frac{1+\xi_i U_i^T U_i^*}{1+\xi_d U_d^T U_d^*} \qquad (\text{with } \left|U_i^T U_d^*\right| = 0) \tag{111}$$

$$S_{max} = \frac{\lambda_{1_{\perp}}}{\lambda_{2_{\parallel}}} = 1+\xi_d U_d^T U_d^* + \xi_i U_i^T U_i^* \qquad (\text{with } U_i^* = hU_d^*) \quad . \tag{112}$$

If, for example we have a three element array with isotropic element patterns and $\xi_d=1$, $\xi_i=1000$, we then have

$$S_{min} = \frac{3001}{4} \cong 750$$

$$S_{max} = 3004 \quad .$$

The eigenvalue spread is just the time constant spread in the array transient response, as can be seen from Equation (7). If, for example, an array with three isotropic elements can accommodate a time constant spread of 3000 then the array would be useful in a signal environment with interference power up to $\xi_i=1000$.

In this section, we have discussed the eigenvalues of Φ'_{CW} for the case of CW signals. In the next section, we point out an interesting relation between the second eigenvalue, λ_2, and the array output signal-to-interference-plus-noise (SINR) for CW signals. Then in Chapter III, Section E, we consider the case of non-zero bandwidth signals.

C. A Relation Between SINR and the Eigenvalues for CW Signals

Here we depart from the main subject of this report, the behavior of the eigenvalues, to discuss an interesting relation between the eigenvalues and the array output SINR.

With the steady state array weight vector in Equation (6) the desired signal component of the array output is

$$\tilde{s}_d(t) = W_{st}^T X_d \quad . \tag{113}$$

The output desired signal power is then ("o" denotes "output")

$$P_{od} = \frac{1}{2} E\{|W_{st}^T X_d|^2\} \quad . \tag{114}$$

Similarly, the output interference and noise powers are

$$P_{oi} = \frac{1}{2} E\{|W_{st}^T X_i|^2\} \tag{115}$$

and

$$P_{on} = \frac{1}{2} E\{|W_{st}^T X_n|^2\} = \frac{\sigma^2}{2} |W_{st}^T|^2 \quad . \tag{116}$$

We define the array output signal-to-interference-plus-noise ratio (SINR) to be

$$SINR = \frac{P_{od}}{P_{oi}+P_{on}} \quad . \tag{117}$$

It has been shown by Ishide and Compton[6] that when there is a desired signal and one interference signal and both are CW, the output SINR from the array may be written

$$\text{SINR} = \xi_d \left(U_d^T U_d^* - \frac{|U_i^T U_d^*|^2}{\xi_i^{-1} + U_i^T U_i^*} \right) \tag{118}$$

The above equation is derived from the matrix inversion lemma[7].

Note that the vector products $U_d^T U_d^*$, $U_i^T U_i^*$ and $U_i^T U_d^*$ which control the behavior of the eigenvalues also appear in the SINR formula. When the signal vectors are orthogonal, i.e., $U_i^T U_d^* = 0$, the SINR in Equation (118) attains its maximum value. This maximum is

$$\text{SINR}_\perp = \xi_d U_d^T U_d^* \quad . \tag{119}$$

From Equation (85) we know that $U_i^T U_d^* = 0$ is also the condition under which λ_2 attains its maximum. On the other hand, when the two signal vectors are parallel, as in Equation (80), we find

$$\begin{aligned} \text{SINR}_{\parallel} &= \xi_d \left[U_d^T U_d^* - \frac{\xi_i |h|^2 (U_d^T U d^*)^2}{1 + \xi_i |h|^2 U_d^T U_d^*} \right] \\ &= \frac{\xi_d U_d^T U_d^*}{1 + \xi_i U_i^T U_i^*} \quad . \end{aligned} \tag{120}$$

Then for the case of strong interference, as given in Equation (71), we have $\text{SINR}_{\parallel} \cong 0$. Therefore, the condition in Equation (80) gives not only minimum λ_2 but also a very small SINR. In conclusion, both λ_2 and the SINR reach their extrema under the same conditions. Hence there appears to be a close relationship between λ_2 and the SINR for the strong interference case.

To find this relationship, we now express the SINR in terms of the eigenvalues. To do so, we first expand the Hermitian matrix Φ'_{cw} in a spectral decomposition[8]. We have

$$[\Phi'_{cw}]^{-1} = \sum_{\ell=1}^{N} \frac{1}{\lambda_\ell} e_\ell^* e_\ell^T \tag{121}$$

where the λ_ℓ's are the eigenvalues and the e_ℓ^*'s are the corresponding eigenvectors of Φ'_{cw}. Recall that Φ'_{cw} is given by Equation (48). Also its first two eigenvectors have been found to be (see Section B, Equation (49))

$$e_1^* = \alpha_1(U_d^* + y_1 U_i^*) = \alpha_1 U_d^* + \beta_1 U_i^* \tag{122}$$

$$e_2^* = \alpha_2(U_d^* + y_2 U_i^*) = \alpha_2 U_d^* + \beta_2 U_i^* \tag{123}$$

and the remaining N-2 eigenvectors are all orthogonal to both U_d^* and U_i^*. Also, the first two eigenvalues are given by Equations (61) and (62) and the remaining N-2 eigenvalues are unity. As we shall see, these unity eigenvalues will not appear in the SINR expression because their associated eigenvectors are orthogonal to both U_d^* and U_i^*.

First we calculate the steady-state weight vector. We assume that the reference signal $\tilde{r}(t)$ is a replica of the desired signal. Then the reference correlation vector is just the desired signal vector, i.e.,

$$S = \gamma U_d^* \tag{124}$$

with γ a proportional constant. From Equation (6), we have

$$W_{st} = \sigma^{-2}[\Phi'_{cw}]^{-1} \gamma U_d^* \quad . \tag{125}$$

Substituting Equation (121) for $[\Phi'_{cw}]^{-1}$, we find that the products between $e_3^T, e_4^T, \cdots, e_N^T$ and U_d^* are zero and do not contribute to the result. Therefore,

$$W_{st} = \sigma^{-2}\gamma\left[\frac{1}{\lambda_1} e_1^*(e_1^T U_d^*) + \frac{1}{\lambda_2} e_2^*(e_2^T U_d^*)\right] \quad . \tag{126}$$

Since the desired signal is CW, we have

$$X_d = \sqrt{\xi_d}\, \sigma\, e^{j(\omega_o t+\psi_d)}\, U_d$$

where $(\sqrt{\xi_d}\,\sigma)^2$ is the input desired signal power P_d, ω_o is the signal frequency and ψ_d is the desired signal phase. We also assume that ψ_d is uniformly distributed between 0 and 2π. Now we can calculate the steady-state desired signal component of the array output from Equation (113). We find

$$\tilde{s}_d(t) = \frac{\gamma\sqrt{\xi_d}}{\sigma} e^{j(\omega_o t+\psi_d)}\left[\frac{1}{\lambda_1}\left|U_d^T e_1^*\right|^2 + \frac{1}{\lambda_2}\left|U_d^T e_2^*\right|^2\right] \quad . \tag{127}$$

From Equation (114), we have the output desired signal power

$$P_{od} = \frac{\xi_d|\gamma|^2}{2\sigma^2}\left[\frac{1}{\lambda_1}\left|U_d^T e_1^*\right|^2 + \frac{1}{\lambda_2}\left|U_d^T e_2^*\right|^2\right]^2 \quad . \tag{128}$$

Similarly we have

$$X_i = \sqrt{\xi_i}\, \sigma\, e^{j(\omega_o t+\psi_i)}\, U_i$$

where $(\sqrt{\xi_i}\sigma)^2$ is the input interference power P_i and ψ_i is the interference phase, also assumed to be uniformly distributed in $[0,2\pi]$. Therefore, we have

$$\tilde{s}_i(t) = \frac{\gamma\sqrt{\xi_i}}{\sigma} e^{j(\omega_o t+\psi_i)}\left[\frac{1}{\lambda_1}\left|U_i^T e_1^*\right|^2 + \frac{1}{\lambda_2}\left|U_i^T e_2^*\right|^2\right] \tag{129}$$

and

$$P_{oi} = \frac{\xi_1 |\gamma|^2}{2\sigma^2} \left[\frac{1}{\lambda_1} \left| U_i^T e_1^* \right|^2 + \frac{1}{\lambda_2} \left| U_i^T e_2^* \right|^2 \right]^2 \quad . \tag{130}$$

The output noise power is given by Equation (116), i.e.,

$$P_{on} = \frac{|\gamma|^2}{2\sigma^2} \left[\frac{1}{\lambda_1^2} \left| U_d^T e_1^* \right|^2 + \frac{1}{\lambda_2^2} \left| U_d^T e_2^* \right|^2 \right] \quad . \tag{131}$$

From Equations (117), (128), (130) and (131) we have

$$\text{SINR} = \frac{\xi_d \left[\frac{\left| U_d^T e_1^* \right|^2}{\lambda_1} + \frac{\left| U_d^T e_2^* \right|^2}{\lambda_2} \right]^2}{\xi_i \left[\frac{\left| U_i^T e_1^* \right|^2}{\lambda_1} + \frac{\left| U_i^T e_2^* \right|^2}{\lambda_2} \right]^2 + \left[\frac{\left| U_d^T e_1^* \right|^2}{\lambda_1^2} + \frac{\left| U_d^T e_2^* \right|^2}{\lambda_2^2} \right]} \tag{132}$$

which gives the SINR in terms of the eigenvalues λ_1, λ_2 and the projections of each signal vector on the eigenvectors.

It is easily seen from Equations (122) and (61) that

$$\begin{aligned} \left| U_d^T e_1^* \right| &= \left| e_1^T U_d^* \right| \\ &= |\alpha_1| \left| U_d^T U_d^* + y_1 U_d^T U_i^* \right| \\ &= \xi_d^{-1} |\alpha_1| (\lambda_1 - 1) \quad . \end{aligned} \tag{133}$$

and similarly

$$\left| U_d^T e_2^* \right| = \xi_d^{-1} |\alpha_2| (\lambda_2 - 1) \tag{134}$$

$$\left| U_i^T e_1^* \right| = \xi_i^{-1} |\alpha_1| (\lambda_1 - 1) \tag{135}$$

$$\left| U_i^T e_2^* \right| = \xi_i^{-1} |\alpha_2| (\lambda_2 - 1) \quad . \tag{136}$$

Putting Equations (133) through (136) into Equation (32), we get

$$\text{SINR} = \frac{\xi_d\left[\dfrac{\xi_d^{-2}|\alpha_1|^2(\lambda_1-1)^2}{\lambda_1} + \dfrac{\xi_d^{-2}|\alpha_2|^2(\lambda_2-1)^2}{\lambda_2}\right]}{\xi_i\left[\dfrac{\xi_i^{-2}|\alpha_1|^2(\lambda_1-1)^2}{\lambda_2} + \dfrac{\xi_i^{-2}|\alpha_2|^2(\lambda_2-1)^2}{\lambda_2}\right]^2 + \left[\dfrac{\xi_d^{-2}|\alpha_1|^2(\lambda_1-1)^2}{\lambda_1^2} + \dfrac{\xi_d^{-2}|\alpha_2|^2(\lambda_2-1)^2}{\lambda_2^2}\right]} \tag{137}$$

The above formula expresses the SINR in terms of the eigenvalues λ_1 and λ_2 and the coefficients $|\alpha_i|$'s and $|\beta_i|$'s. We need these $|\alpha_i|$'s and $|\beta_i|$'s to further simplify the expression.

In Equations (122) and (123), we need α_1 and α_2 as well as y_1 and y_2 (given in Equation (57) and (58)) to specify e_1^* and e_2^* completely. The additional equation needed may be obtained by normalizing e_1^* and e_2^*, i.e., by enforcing

$$e_1^T e_1^* = e_2^T e_2^* = 1 \quad .$$

From Equations (107) and (123), we get

$$e_1^T e_1^* = |\alpha_1|^2 \frac{\lambda_1-1}{\xi_d} + |\beta_1|^2 \frac{\lambda_1-1}{\xi_i} = 1$$

hence

$$\frac{|\alpha_1|^2}{\xi_d} + \frac{|\beta_1|^2}{\xi_i} = \frac{1}{\lambda_1-1} \quad . \tag{138}$$

Similarly we have

$$\frac{|\alpha_2|^2}{\xi_d} + \frac{|\beta_2|^2}{\xi_i} = \frac{1}{\lambda_2-1} \quad . \tag{139}$$

Then from Equations (53) through (58), we have

$$|y_1|^2 = \frac{|\beta_1|^2}{|\alpha_1|^2} = \frac{(a+b)^2}{4\varepsilon_d^2 \left|U_d^T U_i^*\right|^2} = \frac{(\lambda_1 - 1 - \varepsilon_d U_d^T U_d^*)^2}{\varepsilon_d^2 \left|U_i^T U_d^*\right|^2} \tag{140}$$

and

$$|y_2|^2 = \frac{|\beta_2|^2}{|\alpha_2|^2} = \frac{(a-b)^2}{4\varepsilon_d^2 \left|U_d^T U_i^*\right|^2} = \frac{(\lambda_2 - 1 - \varepsilon_d U_d^T U_d^*)^2}{\varepsilon_d^2 \left|U_i^T U_d^*\right|^2} \quad . \tag{141}$$

Substituting Equation (140) into Equation (138), we can solve for $|\alpha_1|^2$ and $|\beta_1|^2$. The results are

$$|\alpha_1|^2 = \frac{1}{\lambda_1 - 1} \left(\frac{1}{\varepsilon_d} + \frac{|y_1|^2}{\varepsilon_i} \right)^{-1} \tag{142}$$

$$|\beta_1|^2 = |y_1|^2 |\alpha_1|^2 \tag{143}$$

with y_1 given in Equation (57). Likewise, by substituting Equation (141) into Equation (139) we have

$$|\alpha_2|^2 = \frac{1}{\lambda_2 - 1} \left(\frac{1}{\varepsilon_d} + \frac{|y_2|^2}{\varepsilon_i} \right)^{-1} \tag{144}$$

and

$$|\beta_2|^2 = |y_2|^2 |\alpha_2|^2 \quad . \tag{145}$$

With the above results, we may express the SINR in terms of the eigenvalues and the signal vectors. The final result is

$$\text{SINR} = \frac{E}{D} \tag{146}$$

where

$$E = \varepsilon_d^{-1}\left[\frac{\lambda_1^{-1}}{\lambda_1}\frac{\varepsilon_i}{\varepsilon_i + \dfrac{(\lambda_1^{-1}-\varepsilon_d U_d^T U_d^*)^2}{\varepsilon_d |U_i^T U_d^*|^2}} + \frac{\lambda_2^{-1}}{\lambda_2}\frac{\varepsilon_i}{\varepsilon_i + \dfrac{(\lambda_2^{-1}-\varepsilon_d U_d^T U_d^*)^2}{\varepsilon_d |U_i^T U_d^*|^2}}\right]^2 \tag{147}$$

$$D = \varepsilon_i^{-1}\left[\frac{\lambda_1^{-1}}{\lambda_1}\frac{\dfrac{(\lambda_1^{-1}-\varepsilon_d U_d^T U_d^*)^2}{\varepsilon_d |U_i^T U_d^*|^2}}{\varepsilon_i + \dfrac{(\lambda_1^{-1}-\varepsilon_d U_d^T U_d^*)^2}{\varepsilon_d |U_i^T U_d^*|^2}} + \frac{\lambda_2^{-1}}{\lambda_2}\frac{\dfrac{(\lambda_2^{-1}-\varepsilon_d U_d^T U_d^*)^2}{\varepsilon_d |U_d^T U_d^*|^2}}{\varepsilon_i + \dfrac{(\lambda_2^{-1}-\varepsilon_d U_d^T U_d^*)^2}{\varepsilon_d |U_i^T U_d^*|^2}}\right]^2$$

$$+ \varepsilon_d^{-1}\left[\frac{\lambda_1^{-1}}{\lambda_1^2}\frac{\varepsilon_i}{\varepsilon_i + \dfrac{(\lambda_1^{-1}-\varepsilon_d U_d^T U_d^*)^2}{\varepsilon_d |U_i^T U_d^*|^2}} + \frac{\lambda_2^{-1}}{\lambda_2^2}\frac{\varepsilon_i}{\varepsilon_i + \dfrac{(\lambda_2^{-1}-\varepsilon_d U_d^T U_d^*)^2}{\varepsilon_d |U_i^T U_d^*|^2}}\right] \tag{148}$$

This general expression is rather unwieldy. But, for the case of very strong interference, the equation reduces to a simple form. If Equations (71) and (72) hold, i.e.,

$$\varepsilon_i U_i^T U_i^* >> \varepsilon_d U_d^T U_d^*$$

and

$$\varepsilon_i >> \varepsilon_d$$

then from our earlier results in Equations (75) and (76), we know that

$$\lambda_1 >> \lambda_2 \quad .$$

Therefore,

$$E \cong \varepsilon_d^{-1} \left[\frac{\lambda_2^{-1}}{\lambda_2} \frac{\varepsilon_i}{\varepsilon_i + \dfrac{(\lambda_2^{-1} - \varepsilon_d U_d^T U_d^*)^2}{\varepsilon_d \left| U_i^T U_d^* \right|^2}} \right]^2 \tag{149}$$

and

$$D \cong \varepsilon_d^{-1} \left[\frac{\lambda_2^{-1}}{\lambda_2^2} \frac{\varepsilon_i}{\varepsilon_i + \dfrac{(\lambda_2^{-1} - \varepsilon_d U_d^T U_d^*)^2}{\varepsilon_d \left| U_i^T U_d^* \right|^2}} \right] \tag{150}$$

where the first term in Equation (147) involving λ_1 is negligible and the first term in Equation (148) is also neglected because it involves ε_i^{-1}, which is much smaller than the second term, proportional to ε_d^{-1}. Thus,

$$SINR = (\lambda_2^{-1}) \frac{\varepsilon_i}{\varepsilon_i + \dfrac{(\lambda_2^{-1} - \varepsilon_d U_d^T U_d^*)^2}{\varepsilon_d \left| U_i^T U_d^* \right|^2}} \quad . \tag{151}$$

The above expression can be further simplified by recognizing that

$$\frac{\varepsilon_i}{\dfrac{(\lambda_2^{-1} - \varepsilon_d U_d^T U_d^*)^2}{\varepsilon_d \left| U_d^T U_d^* \right|^2}} \cong \varepsilon_i = 1$$

under Equations (71) and (72). Therefore we have

$$SINR \cong \lambda_2^{-1} \quad . \tag{152}$$

This remarkably simple result is valid for arbitrary element spacings, element patterns and signal arrival angles, but only for CW signals. The formula is interesting because it tells us that when the interference is much stronger than the desired signal, λ_2 controls not only the transient response of the array but also the steady-state SINR performance.

Much recent work has been directed at the problem of choosing element patterns in an adaptive array. The goal of this work is to find element patterns for which the SINR does not vary widely as the signal arrival angles change. We note, however, that because of Equation (152), choosing element patterns to minimize the SINR variation also minimizes the variation in both λ_2 and the eigenvalue spread.

We now return to the main subject of this report and discuss the behavior of the eigenvalues in typical situations.

CHAPTER III
RESULTS AND DISCUSSION

We have determined the N eigenvalues of the covariance matrix for an N-element adaptive array with a CW desired signal and a CW interference signal incident on it. We have also related the eigenvalues to the array output SINR, as given in Equations (146) and (152).

In this Chapter, we shall discuss the behavior of the eigenvalues and relate their values to the signal strengths (ξ_d and ξ_i), the number of elements, the element spacings, the element patterns and the signal bandwidths.

To illustrate the behavior of the eigenvalues, we first present Figure 4, which shows a typical set of eigenvalues; it shows all three eigenvalues (λ_1, λ_2 and λ_3) versus the interference angle θ_i for a three-element array. The desired signal angle is arbitrarily fixed at θ_d=45° and the interference angle is varied between 0° and 360°. Both signals are CW. The elements are assumed isotropic and a half-wavelength apart (D_1=0, D_2=0.5λ_o, D_3 = 1.0λ_o). The signal-to-noise ratios are ξ_d=1 and ξ_i=10.

From Figure 4, we observe the following:

1) λ_1, the largest eigenvalue, is always larger than 31. This minimum of λ_1 is determined by $1+\xi_i U_i^T U_i^*$ from Equation (93).

2) λ_2, the middle eigenvalue, varies between 1 and 4, i.e., $1 \leq \lambda_2 \leq 1 + \xi_d U_d^T U_d^*$ from Equation (103).

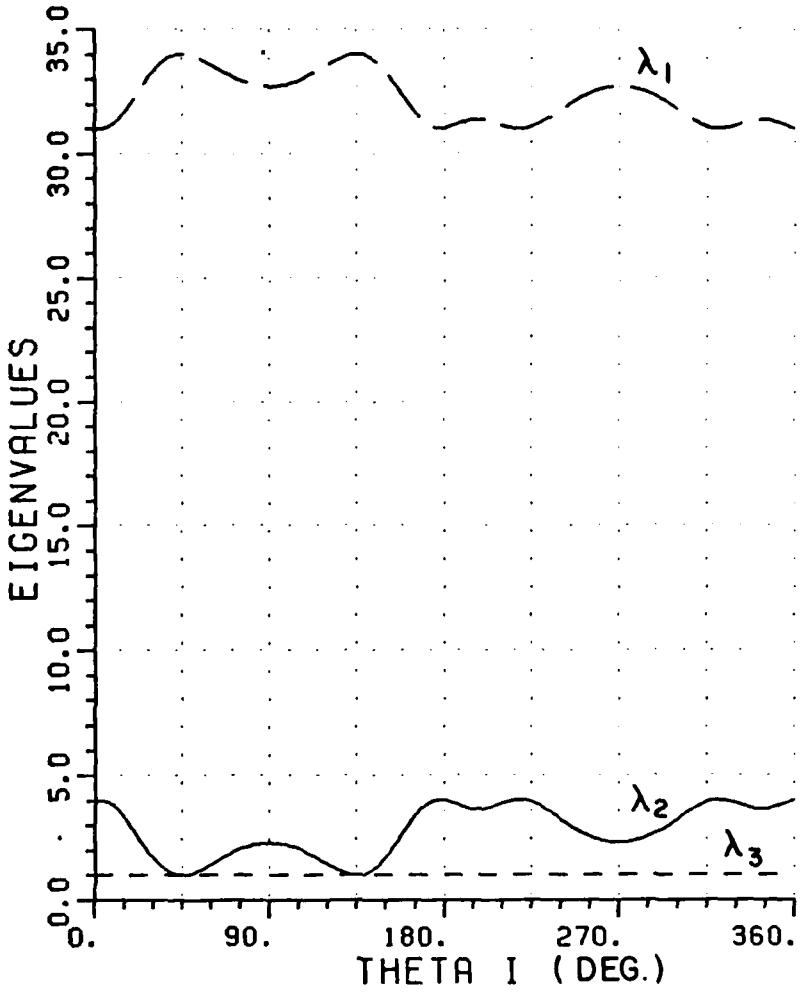

Figure 4. Eigenvalues vs θ_i
SNR=1.0
INR=10
BD=0.0 (DESIRED SIGNAL BANDWIDTH)
BI=0.0 (INTERFERENCE BANDWIDTH)
THETA D = 45 DEGREES
3-ELEMENT ARRAY WITH HALF-WAVELENGTH SPACINGS.

3) $\lambda_3=1$.

4) λ_1 has a range of variation equal to 3, i.e.,

$$\lambda_{1_{max}} - \lambda_{1_{min}} = 34-31 = 3.$$

This range is determined by the weaker signal (the desired signal) and has value $\varepsilon_d U_d^T U_d^*$ (from Equation (98)). Also we find that $\lambda_{1_{max}} = \lambda_{1_{\parallel}} = 34$, $\lambda_{1_{min}} = \lambda_{1_{\perp}} = 31$.

5) λ_2 also has a range of 3, i.e., $\varepsilon_d U_d^T U_d^*$. (From Equation (103)).

6) The eigenvalue spread S has extrema

$$S_{max} = 1+\varepsilon_i U_i^T U_i^* + \varepsilon_d U_d^T U_d^* = 34 \qquad \text{(Equation (112))}$$

$$S_{min} = \frac{1+\varepsilon_i U_i^T U_i^*}{1+\varepsilon_d U_d^T U_d^*} = \frac{31}{4} = 7.75 \qquad \text{(Equation (111)).}$$

7) The sum of the three eigenvalues is constant, i.e.,

$$\lambda_1+\lambda_2+\lambda_3 = N(\varepsilon_i+\varepsilon_d+1) = 36 \quad .$$

From 1) and 2), we see that the levels of the eigenvalues are determined by the signal strengths, namely, λ_1 by ε_i and λ_2 by ε_d. λ_3 is always constant (unity). Points 4) and 5) illustrate how the ranges of the eigenvalues are controlled by the weaker signal, in this case the desired signal. The graph also shows that the eigenvalue variation is symmetrical around $\theta_i=90°$ and 279°, i.e.,

$$\lambda(90°-\delta) = \lambda(90°+\delta): \quad \lambda(279°-\delta) = \lambda(270°+\delta) \quad .$$

This symmetry comes from the fact that

$$U_i^*(\theta_i) = U_i^*(180°-\theta_i).$$

With this background, we now discuss the effect of each of the system parameters separately. We start with the signal strengths.

A. The Effect of Signal Strength

We first show how eigenvalues are affected by the desired signal strength, ξ_d. Figure 5 shows the three eigenvalues with $\xi_d=3$ and with all other parameters the same as in Figure 4. (Figure 4 was for $\xi_d=1$).

Comparing the two plots, we find

1) The minimum value of λ_1 is still 31, i.e., the minimum value of λ_1 does not depend on ξ_d, as can be seen from Equation (93).

2) λ_2 has minimum 1 and varies between 1 and 10. The bounds on λ_2 are from Equation (103) again.

3) λ_3 remains constant (unity).

4) λ_1 has a larger range of variation, 9 in this case, which is $\xi_d U_d^T U_d^*$ (or $N\xi_d$). Also we see that

$$\lambda_{1_{max}} = \lambda_{1_{\parallel}} = 40, \quad \lambda_{1_{min}} = \lambda_{1_{\perp}} = 31.$$

5) λ_2 also has a larger range of 9, we also have

$$\lambda_{1_{max}} = \lambda_{2_{\perp}} = 10, \quad \lambda_{2_{min}} = \lambda_{2_{\parallel}} = 1.$$

6) The eigenvalue spread has extrema

$$S_{max} = 40 \qquad \text{(from Equation (112))}$$

$$S_{min} = \frac{31}{10} = 3.1 \qquad \text{(from Equation (111))}$$

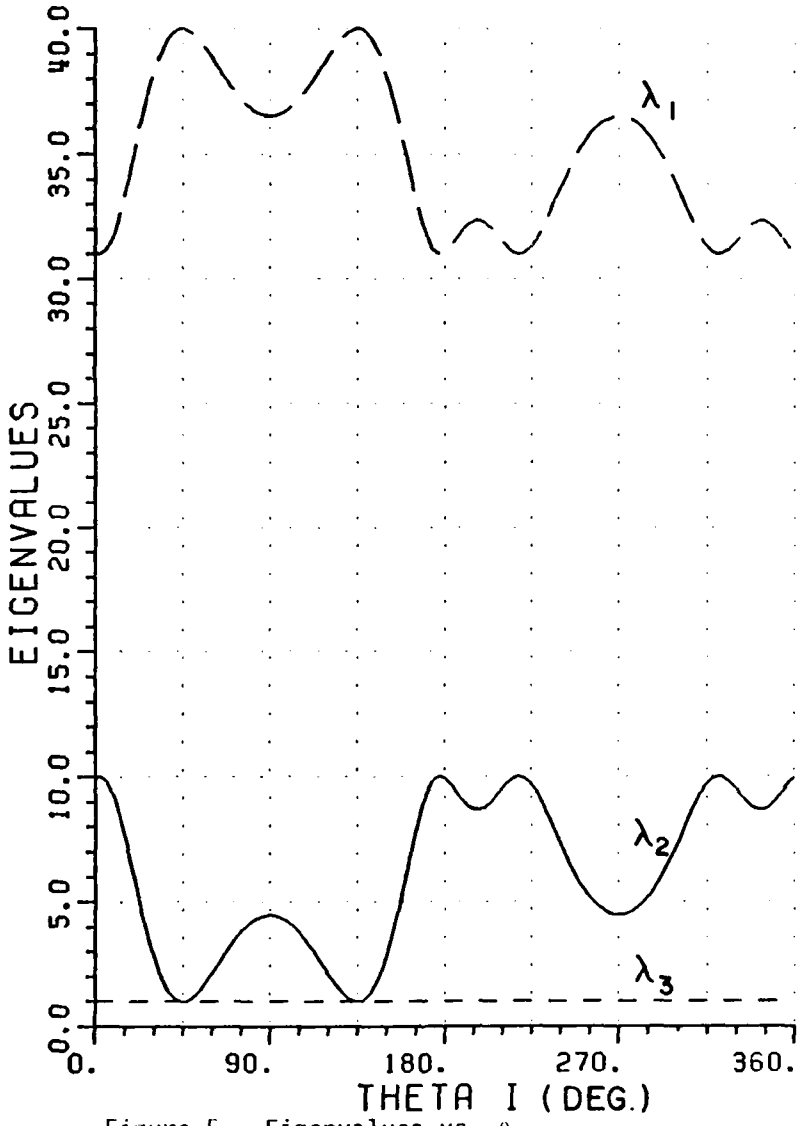

Figure 5. Eigenvalues vs. θ_i
SNR=3.0
INR=10.
BD=0.0
BI=0.0
THETA D = 45 DEGREES
3-ELEMENT ARRAY WITH HALF-WAVELENGTH SPACINGS.

7) The sum of the three eigenvalues is a constang equal to, in this case, 42.

From the above observations, we see that the desired signal strength ξ_d affects the range of variation of λ_1 and λ_2. The range is proportional to ξ_d. In addition, the increase in ξ_d substantially reduces S_{min} (from 7.75 to 3.1). At the same time, increasing ξ_d makes S_{max} to increase (from 34 to 40). Therefore, tripling ξ_d reduces S_{min} more than by a half and only causes S_{max} to increase less than 20%.

The previous example was for the case of weak interference (ξ_i=10). We now consider how ξ_d affects the eigenvalues when ξ_i is much stronger. We let ξ_i=1000 and calculate λ_1 for three different ξ_d's (ξ_d=1, 10 and 100). The result is shown in Figure 6. We see clearly that λ_1 is little affected by the increase in ξ_d for strong interference. Thus, the larger eigenvalue λ_1 can be regarded as independent of ξ_d as long as $\xi_i/\xi_d \geq 10$ and $\xi_i \geq 1000$.

In Figure 7, we show λ_2 calculated for two ξ_d values with all other parameters the same as in Figure 6. Clearly, λ_2 depends very much on ξ_d. Acutally, for ξ_d=10 is just a magnified version of the case ξ_d=1.

Next, we discuss the effect of interference strength. First, we show that λ_1, the largest eigenvalue, depends mainly on the interference. In Figure 8, we have λ_1 plotted against θ_i for three interference strengths, ξ_i=100, 1000 and 10000 with all other parameters the same as in Figure 4. It clearly shows how for strong interference the largest eigenvalue λ_1 is a constant, $3\xi_i$, as a function of θ_i. To show the exact relation between λ_1 and ξ_i, we present Figure 9, which is an enlarged version of $\lambda_1(\theta_i)$ for ξ_i=100. The percentage change of λ_1 from its minimum (301) to maximum (304) is so small that λ_1 can

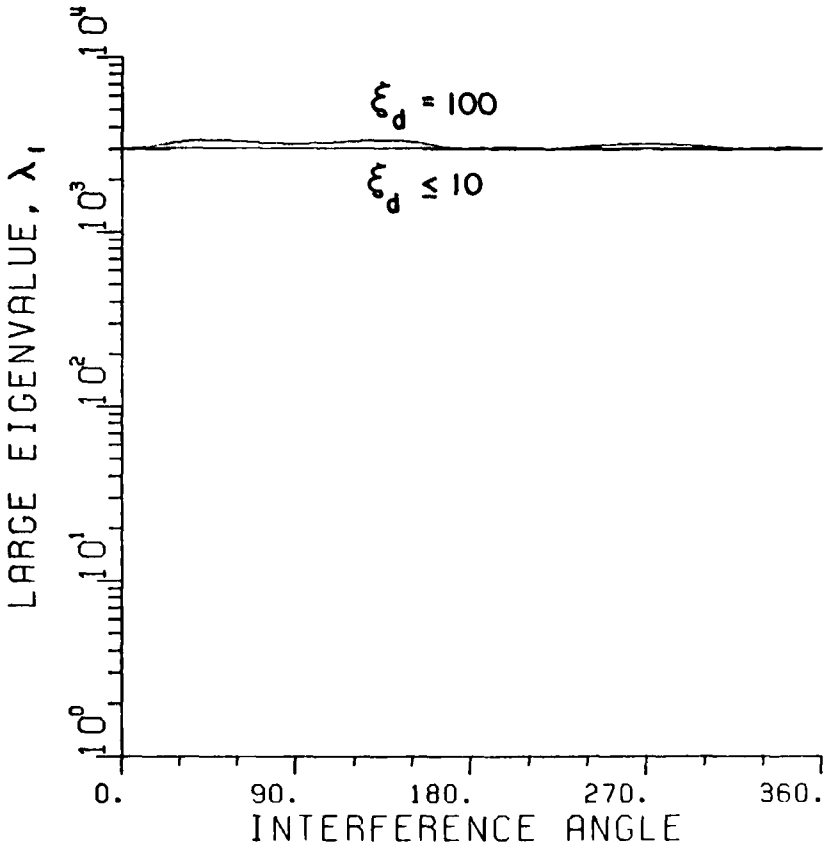

Figure 6. Effect of SNR under strong interference
SNR IS VARIED.
INR=1000.
BD=0.0.
BI=0.0.
THETA D = 45 DEGREES.
3-ELEMENT ARRAY WITH HALF-WAVELENGTH SPACING.

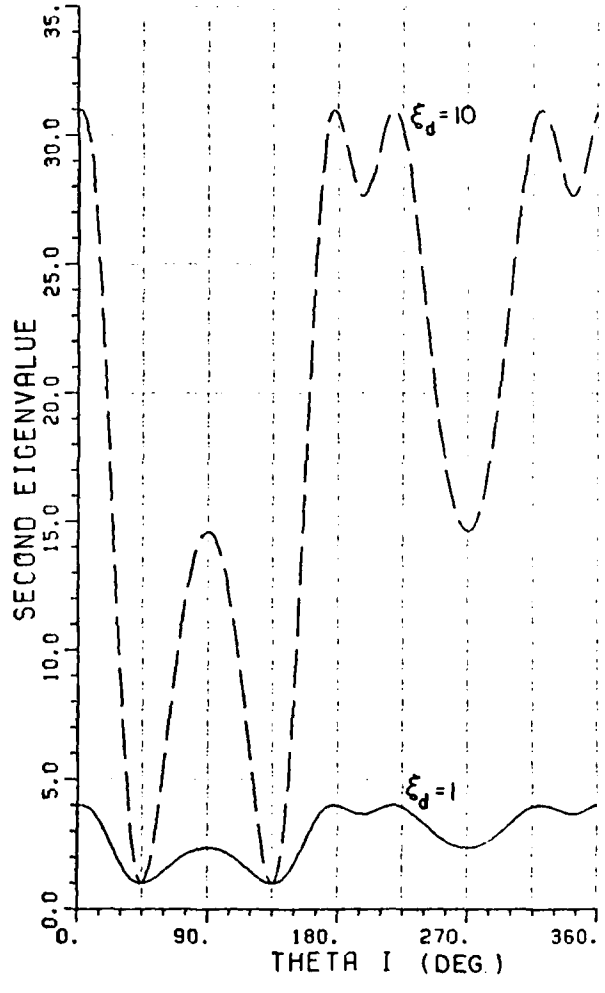

Figure 7. λ_2 vs. θ_i for ξ_d=1 and ξ_d=10.
INR=1000.
BD=0.
BI=0
θ_i=45°.
3-ELEMENT ARRAY WITH HALF WAVELENGTH SPACING.

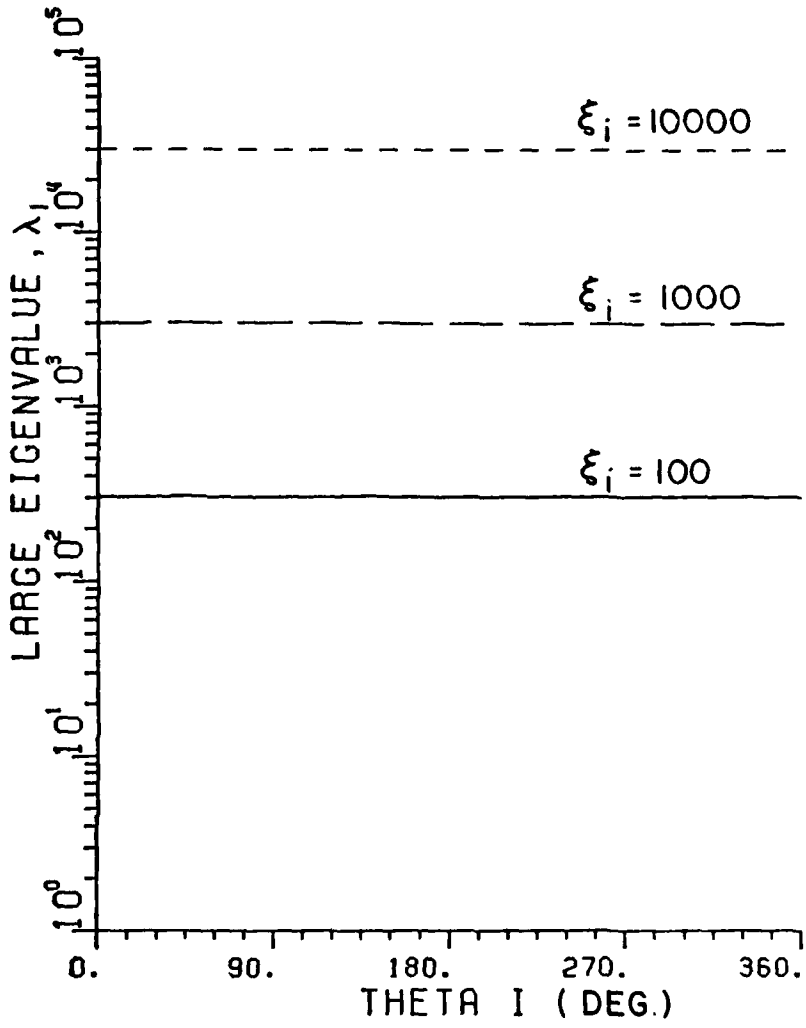

Figure 8. λ_1 for strong interference.
SNR=1.; INR=1000, 1000, 10000
BD=0.000; BI=0.000;
THETA D=45.DEGREES:
3-ELEMENT ARRAY WITH HALF-
WAVELENGTH SPACING.

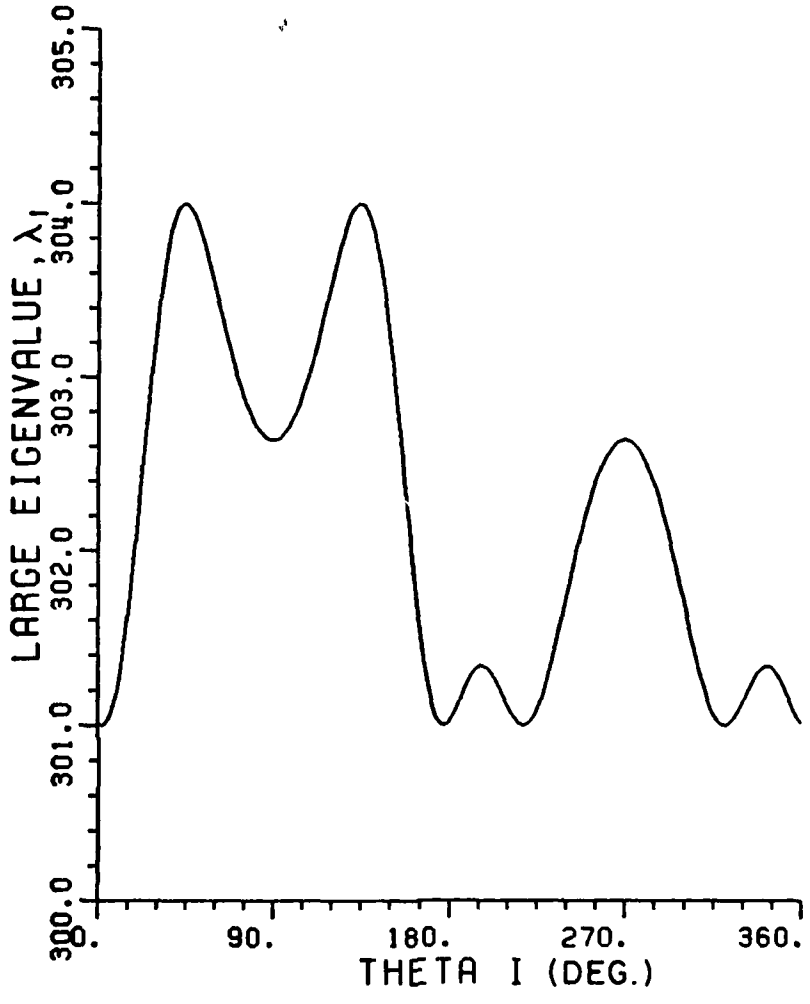

Figure 9. Magnified λ_1 for ξ_i=100.

SNR=1.; INR=100;
BD=0.000; BI=0.000;
THETA D=45. DEGREES
3-ELEMENT ARRAY WITH HALF-
WAVELENGTH SPACING.

indeed be considered as a constant proportional to ε_i, as Figure 8 indicates.

We now show how the large eigenvalue λ_1 behaves with weak interference. In Figure 10, we show λ_1 for ε_i=0.01, 0.1 and 1 with the other parameters the same as in Figure 4. As may be seen, λ_1 is nearly constant for ε_i=0.01. For $\varepsilon_i \ll \varepsilon_d$, we have

$$\lambda_1 \cong 1+3\varepsilon_d \qquad \text{(from Equation (93))}.$$

Then as ε_i increases, λ_1 also increases. When $\varepsilon_i \gg \varepsilon_d$, we have

$$\lambda_1 \cong 1+3\varepsilon_i \qquad \text{(from Equation (93))}.$$

Thus, λ_1 depends on ε_d when $\varepsilon_i \ll \varepsilon_d$ because λ_1 depends on the stronger of the two incoming signals. Once ε_i becomes larger than ε_d, λ_1 is controlled by ε_i.

Now consider how λ_2 behaves as ε_i is varied. Figure 11 shows λ_2 calculated for various interference powers from ε_i=0.01 to 100 for the same array. We first note that λ_2 approaches an upper bound as ε_i increases. This upper bound is the curve of output SINR less one (see Equation (152)). In the figure, the top curve shows λ_2 for ε_i=100 and also gives the output SINR from the array (read from the right-hand side scale). Note that the curve for ε_i=10 deviates little from the ε_i=100 curve, so we conclude that the approximation

$$\lambda_2 = \text{SINR}+1$$

causes little error as long as $\varepsilon_i \geq 10\varepsilon_d$.

When ε_i=0.01 or less, the second eigenvalue is essentially unity, as shown. In this case, the array behaves as if there is only one signal present, the desired signal. Hence there is only one eigenvalue

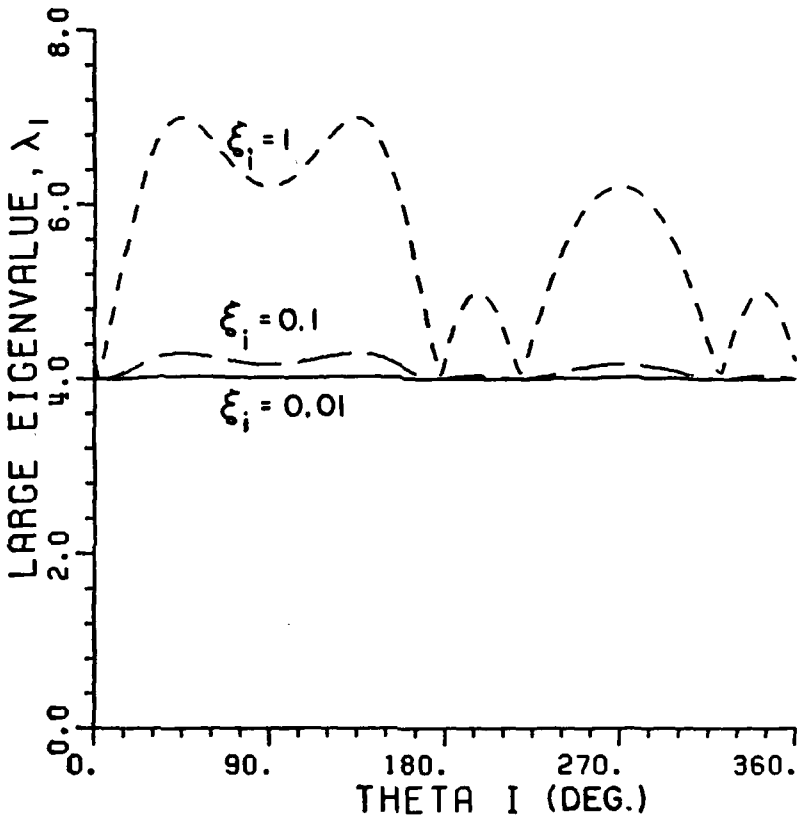

Figure 10. λ_1 for weak interference.
SNR=1.; INR=0.01, 0.1, 1
BD=0.000; BI=0.000;
THETA D= 45.DEGREES.
3-ELEMENT ARRAY WITH HALF-WAVELENGTH SPACING.

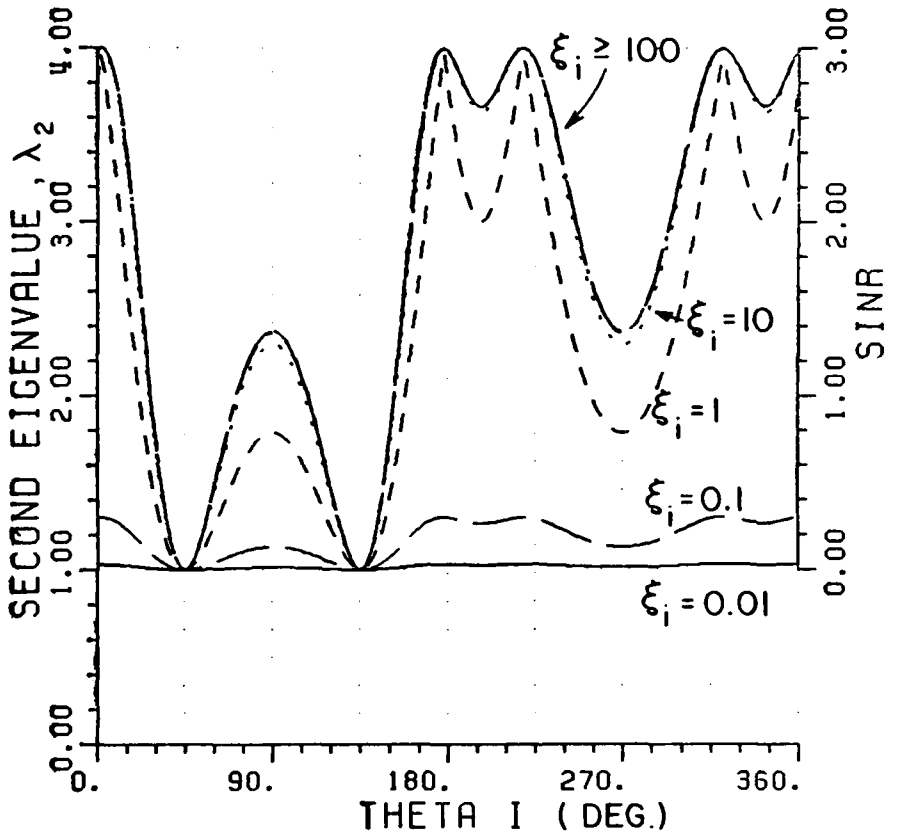

Figure 11. λ_2 for different ξ_i.

SNR=1.0
INR IS CHANGED FROM
0.01 TO 10000
BD=0.0
BI=0.0
THETA D=45 DEGREES
3-ELEMENT ARRAY WITH
UNIFORM HALF-WAVE
LENGTH SPACING.

different from unity, λ_1. The output SINR for this case is $\varepsilon_d U_d^T U_d^*$, from Equation (118). λ_2 does not approximate 1+SINR because the condition $\varepsilon_i U_i^T U_i^* >> \varepsilon_d U_d^T U_d^*$ is not met. Thus the curves in Figure 10 do not indicate the SINR behavior for cases where $\varepsilon_i \leq 1$.

From Equation (109), we see that the eigenvalue spread increases with increased ε_i because λ_2 is bounded by 1+SINR and λ_1 is proportional to ε_i. The extrema of the eigenvalue spread S are

$$S_{min} = \frac{1+N\varepsilon_i}{1+N\varepsilon_d} \cong \frac{N\varepsilon_i}{1+N\varepsilon_d}$$

$$S_{max} = 1+N\varepsilon_i+N\varepsilon_d \cong N\varepsilon_i \quad .$$

These extrema also increase with increased ε_i. The problem of eigenvalue spread arises when the interference is so strong ($\varepsilon_i/\varepsilon_d \geq 10^3$) that the array cannot accomodate the widely separated eigenvalues (or the widely separated time constants). When ε_i is small, the eigenvalue spread is small and causes no problem. Thus we are interested in the eigenvalue behavior under strong interference. For large ε_i, λ_1 is essentially constant as signal angles and ε_d vary, so we shall not consider λ_1 any further. Moreover, λ_3 is unity for CW signals, so the only eigenvalue that varies with signal angle is λ_2. In the following two sections, we shall concentrate on λ_2 and discuss the effects of the number of elements, signal bandwidth, etc., on the behavior of λ_2.

B. The Effect of the Number of Elements

In Figure 12, we show three plots of λ_2 (as well as SINR) versus θ_i with N=2, 3 and 4. In general, we obtain better output SINR with more elements because the larger N, the greater the array gain. Correspondingly, λ_2 increases with increased N. Moreover, as the number of elements is increased, the eigenvalue spread also increases. For example, the extrema of the eigenvalue spread are:

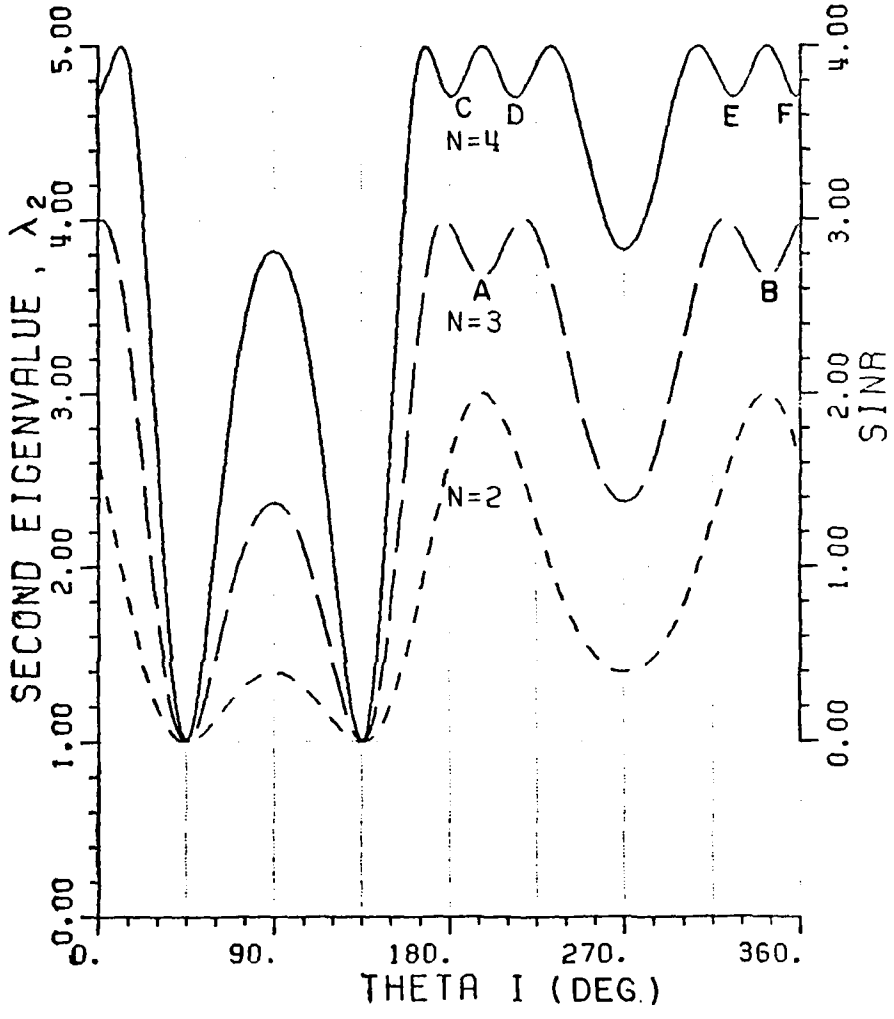

Figure 12. Relation between λ_2 and N.

SNR=1.0
INR=1000.
BD=0.0
BI=0.0
THETA D=45 DEGREES
NUMBER OF ELEMENTS IS CHANGED.
UNIFORM HALF-WAVELENGTH SPACINGS.

$$S_{2_{min}} = \frac{2001}{3} \cong 670 \qquad S_{2_{max}} = 2003$$

$$S_{3_{min}} = \frac{3001}{4} \cong 750 \qquad S_{3_{max}} = 3004$$

$$S_{4_{min}} = \frac{4001}{5} \cong 800 \qquad S_{4_{max}} = 4005$$

where subscripts 2, 3 and 4 indicate the number of elements. We see from Equation (111) that for isotropic elements

$$\lim_{N\to\infty} S_{N_{min}} = \frac{\xi_i}{\xi_d}$$

because $U_i^T U_i^* = U_d^T U_d^* = N$. Thus, the minimum eigenvalue spread increases to a limit, ξ_i/ξ_d, with increasing number of elements

Note that with four elements, there are four local minima indicated by points C, D, E and F in Figure 12. For three elements, there are only two such relative minima (indicated by points A and B). Thus, as we increase the number of elements, the number of these minima will also increase. The value of λ_2 at these minima may decrease if we change the array parameters, such as the element spacings. These minima may sometimes drop to unity. When this happens, there is a corresponding null in the SINR. This situation is due to the presence of a grating null in the antenna pattern[6]. In addition, the maxima on these curves correspond to the cases where $U_i^T U_d^* = 0$, which as we know from Equation (118), results in maximum output SINR.

C. The Effect of Element Spacing

Since the covariance matrix depends on the interelement phase shifts, which in turn depend on the interelement spacings, we expect the interelement spacings to have an important role on the eigenvalue behavior.

We begin by considering λ_2 for a two element array with several values of separation D_2 between elements. The elements are assumed to be isotropic. A series of plots of λ_2 will be shown. The first of these, Figure 13, shows λ_2 calculated for four separations, D_2=0.05λ_o, 0.1λ_o, 0.2λ_o and 0.3λ_o as indicated. In later graphs, D_2 is further increased so we are able to see the gradual variation of λ_2 with D_2. As before, ε_d=1, ε_i=1000, θ_d=45° and both signals are CW.

From Figure 13, we see that for very small separation (D_2=0.05 λ_o), λ_2 stays nearly constant at unity. This result indicates that the output SINR of the array is poor for every θ_i. Because the small separation cannot provide enough phase shift between elements, the array is not able to produce a satisfactory SINR.

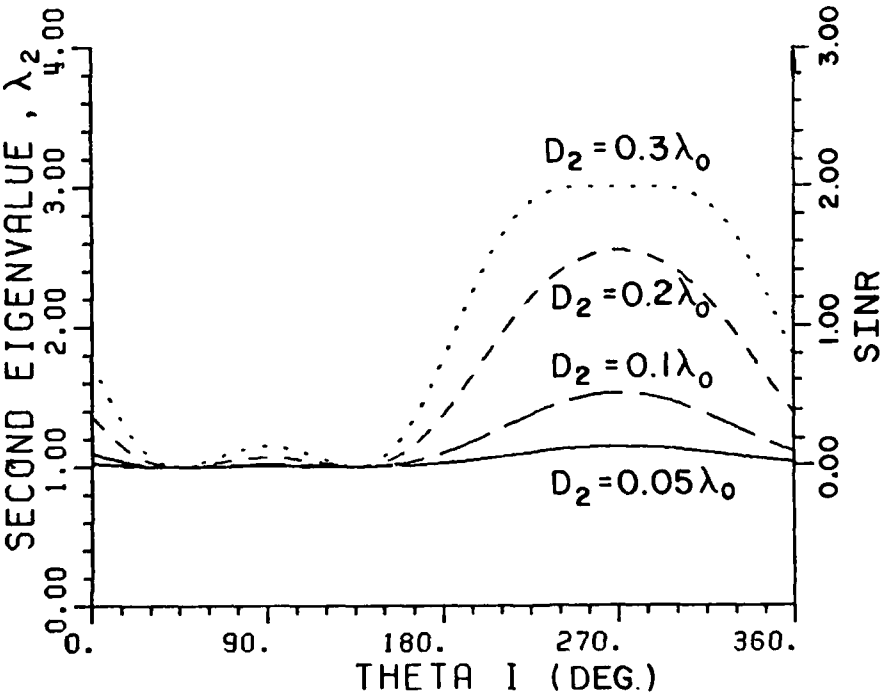

Figure 13. Effect of element spacings (D_2 is varied)
SNR-1 , INR-1000, BD-0.000, BI-0.000,
THETA D=45 DEGREES
2-ELEMENT ARRAY.

Putting N=2 in the SINR formula in Equation (118), we have the SINR for the two element array as

$$SINR_2 = 2\varepsilon_d \sin^2 \frac{\phi_{i_2} - \phi_{d_2}}{2} \tag{153}$$

where we have used

$$U_d = \begin{bmatrix} 1 \\ e^{-j\phi_{d_2}} \end{bmatrix}, \quad U_i = \begin{bmatrix} 1 \\ e^{-j\phi_{i_2}} \end{bmatrix}$$

and

$$\phi_{d_2} = \frac{2\pi D_2}{\lambda_o} \sin\theta_d, \quad \phi_{i_2} = \frac{2\pi D_2}{\lambda_o} \sin\theta_i .$$

Thus, for $D_2 \leq 0.05\lambda_o$ the phase shifts ϕ_{d_2} and ϕ_{i_2} and hence the SINR are small.

The fact that $\lambda_2=1$ also means that the eigenvalue spread S is large for all θ_i. For $D_2=0.05\lambda_o$, we have

$$S_{min} \cong S_{max} \cong 2000.$$

As the separation increases from $0.1\lambda_o$ to $0.3\lambda_o$ in Figure 13, we see that λ_2 also increases. In other words, we have better SINR as well as decreased eigenvalue spread with increased element separation. From the figure, we see that with a spacing $0.2\lambda_o$, the two-element array is able to null interference adequately in the sector $180° \leq \theta_i \leq 360°$ for $\theta_d=45°$ if the minimum required output SINR from the array is not higher than 0.4 (-4 dB).

The next graph, Figure 14, shows λ_2 for the same conditions as in Figure 13 except that $D_2=0.4\lambda_o$, $0.5\lambda_o$ and $0.6\lambda_o$. The SINR improves in the sector $0° < \theta_i < 180°$ with increased separation but degrades in the sector $180° < \theta_i < 360°$. In particular, for $D_2=0.6\lambda_o$, the SINR is low when the interference is coming from $240° < \theta_i < 300°$. For still larger

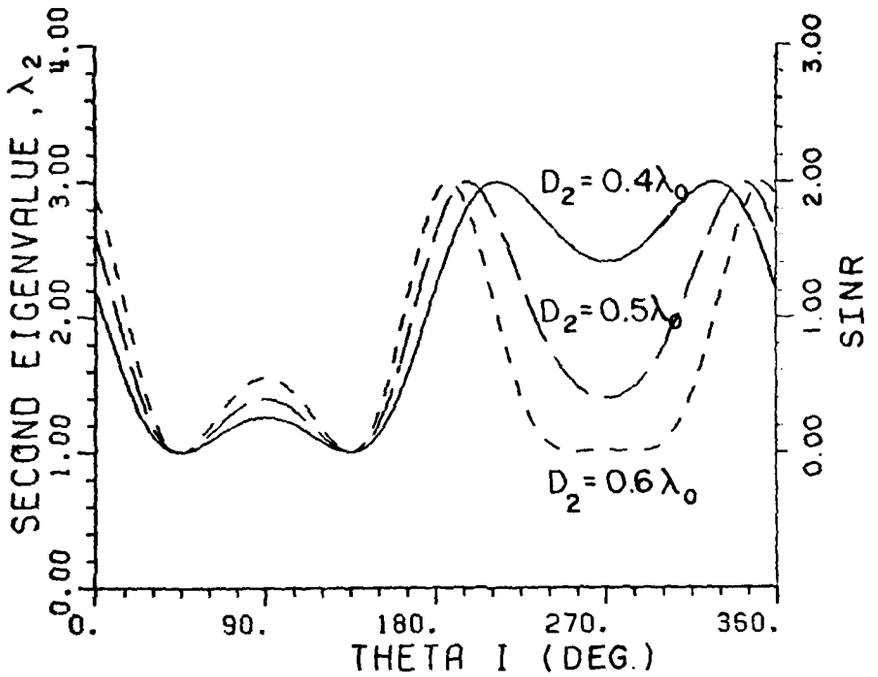

Figure 14. Effect of element spacing (D_2=0.4λ_0, 0.5λ_0 and 0.6λ_0). SNA=1., INR=1000., BD=0.000, BI=0.000, THETA D=45. DEGREES; 2-ELEMENT ARRAY.

separations, the array starts to have grating nulls. Figure 15 illustrates this phenomenon. The graph shows λ_2 for D_2=0.7λ_0, 0.8λ_0 and 0.9λ_0, respectively. For D_2=0.7λ_0, there are two grating nulls around θ_i=225° and θ_i=315°. As the separation is increased, the grating nulls move in opposite directions as indicated. In Figure 16, λ_2 is plotted with D_2=1.6λ_0 and 1.7λ_0. λ_2 exhibits fast fluctuations between its extrema and the SINR has sharper lobes and more grating nulls.

In conclusion, for two isotropic elements, the number of grating nulls and the number of minima and/or maxima increase with increased element separation. With very small separation, such as for D_2 0.05λ_0, the eigenvalue spread is roughly $N\xi_i$ which is high for strong interference. When the separation is large enough to produce grating nulls, it also gives large eigenvalue spread.

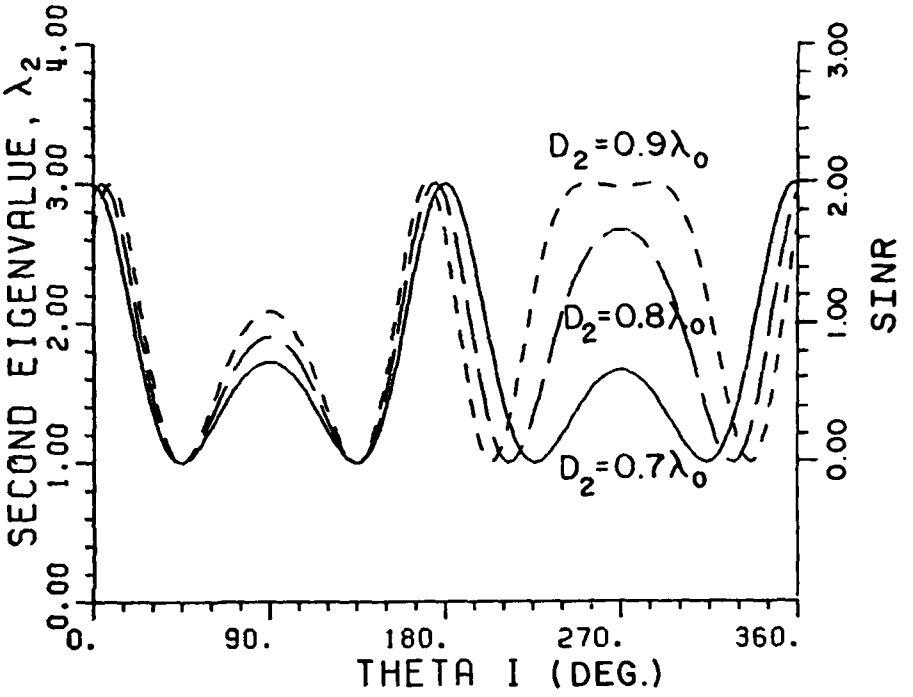

Figure 15. Effect of element spacing ($D_2=0.7\lambda_o$, $0.8\lambda_o$ and $0.9\lambda_o$).
SNR=1., INR=1000., BD=0.000, BI=0.000, THETA D=45. DEGREES, 2-ELEMENT ARRAY.

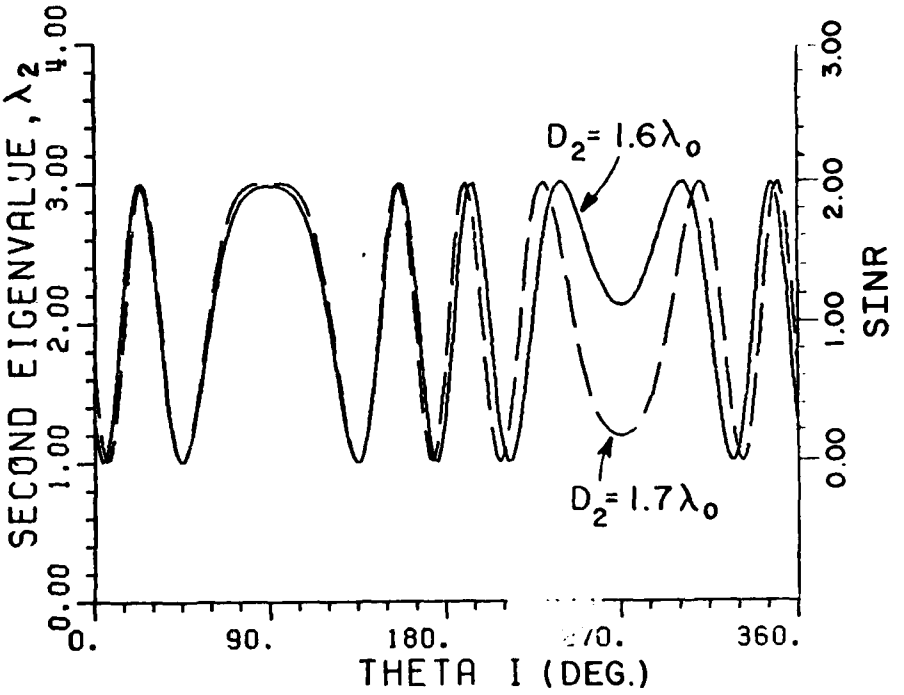

Figure 16. Effect of element spacing (D_2=1.6λ_o and 1.7λ_o).
SNR=1., INR=1000., BD=0.000, BI=0.000,
THETA D=45. DEGREES, 2-ELEMENT ARRAY.

We now show how λ_2 varies with interelement spacing for a three element array. In order to make comparisons among various cases, we first fix the total length of the array, D_3, and then change D_2 by moving the center element.

Figure 17 shows λ_2 for $D_2=0.1\lambda_o$, $0.3\lambda_o$ and $0.5\lambda_o$ with D_3 kept constant at λ_o. From the figure, we see the least desirable choice is $D_2=0.1\lambda_o$ because it gives very low SINR around $\theta_i=220°$ and $\theta_i=340°$. Considering the SINR output in the sector $0°\leq\theta_i\leq180°$, the three cases give nearly identical performance. However, in the sector $180°\leq\theta_i\leq 360°$, the case with $D_2=0.3\lambda_o$ does not have as deep as a null as the case $D_2=0.5\lambda_o$ or $D_2=0.1\lambda_o$. This fact suggests that the equally spaced array may not be the best choice in certain conditions.

Next, we keep D_2 fixed and vary the total length D_3. We arbitrarily choose $D_2=0.3\lambda_o$ and let D_3 change from $0.5\lambda_o$ to $1.2\lambda_o$ and to $2\lambda_o$. The eigenvalue, λ_2, for this three cases is shown in Figure 18. In general, increasing the total spacing gives higher SINR and gives sharper nulls around $\theta_i=\theta_d$ and $\theta_i=180°-\theta_d$. However, from Figure 18 we see that around points A and A' the case $D_2=2\lambda_o$ gives lower SINR than the case with $D_2=1.2\lambda_o$. Thus, with increased total spacing the array will have additional SINR drops such as those around A and A' in the figure.

D. The Effect of Element Patterns

In the previous sections, we have assumed that the elements are isotropic. We shall now illustrate how element patterns affect the eigenvalues.

With isotropic elements, and with the interference much stronger than the desired signal, the largest eigenvalue, λ_1, exhibits little variation as the signal angles vary. For non-isotropic elements, however, λ_1 is no longer constant. Also, the behavior of the middle

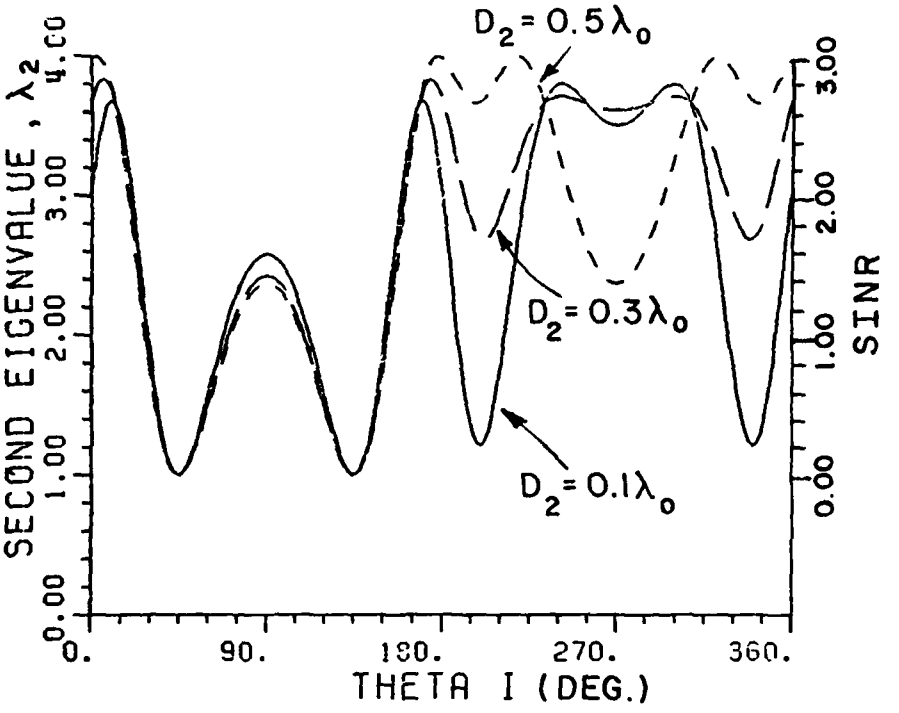

Figure 17. Effect of element spacing (D_2 is varied, $D_3=1\lambda_o$).

SNR=1.0
INR=1000.
BD=0.0.
BI=0.0.
THETA D=45 DEGREES
THE ELEMENT SPACINGS ARE CHANGED.

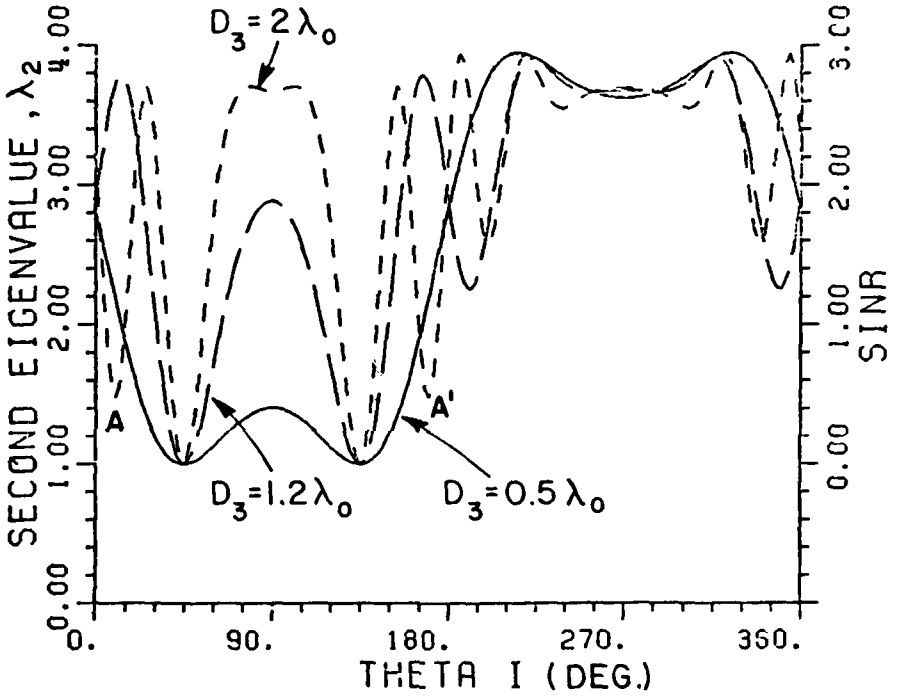

Figure 18. Effect of element spacings ($D_2=0.3\lambda_o$, D_3 is varied).
SNR=1., INR=1000., BD=0.000, BI=0.000
THETA D=45. DEGREES
3-ELEMENT ARRAY.

eigenvalue, λ_2, is changed. We shall use a three element array of dipoles spaced a half-wavelength apart to illustrate these effects.

Let us assume each of the elements is a short dipole with a cosine pattern of the form

$$f_\ell(\theta) = \cos(\theta+\delta_\ell)$$

for ℓ=1,2,3. Initially, we shall assume all three elements have their pattern maxima at broadside, i.e.,

$$\delta_\ell = 0$$

for ℓ=1,2,3. Then, all elements also have nulls at θ=90° and 270°. First we consider the case where the interference is weak, i.e., let ξ_d=1 and ξ_i=10. Also, we let θ_d=45° as usual. The resultant eigenvalues (λ_1,λ_2 and λ_3) are shown in Figure 19.

Comparing Figure 19 with Figure 4 (calculated for isotropic elements), we see that the first difference is in the largest eigenvalue, λ_1. The range of variation of λ_1 in Figure 19 is much larger than that in Figure 4. With cosine elements, we have

$$\lambda_{1_{max}} = 31, \quad \lambda_{1_{min}} = \lambda_1(\theta_i=90°, \text{ or } 270°) = 2.5 .$$

Notice that $\lambda_{1_{min}}$ occurs when the interference is arriving in the pattern nulls at θ_i=90° or 270°. In the vicinity of these two interference angles, we have

$$\xi_i U_i^T U_i^* << \xi_d U_d^T U_d^*$$

so the array behaves as if only one (the desired) signal is present. Hence λ_1 is just $1+3\xi_d|f(\theta_d)|^2 = 1 + \frac{3}{2} = \frac{5}{2}$ which checks with the figure.

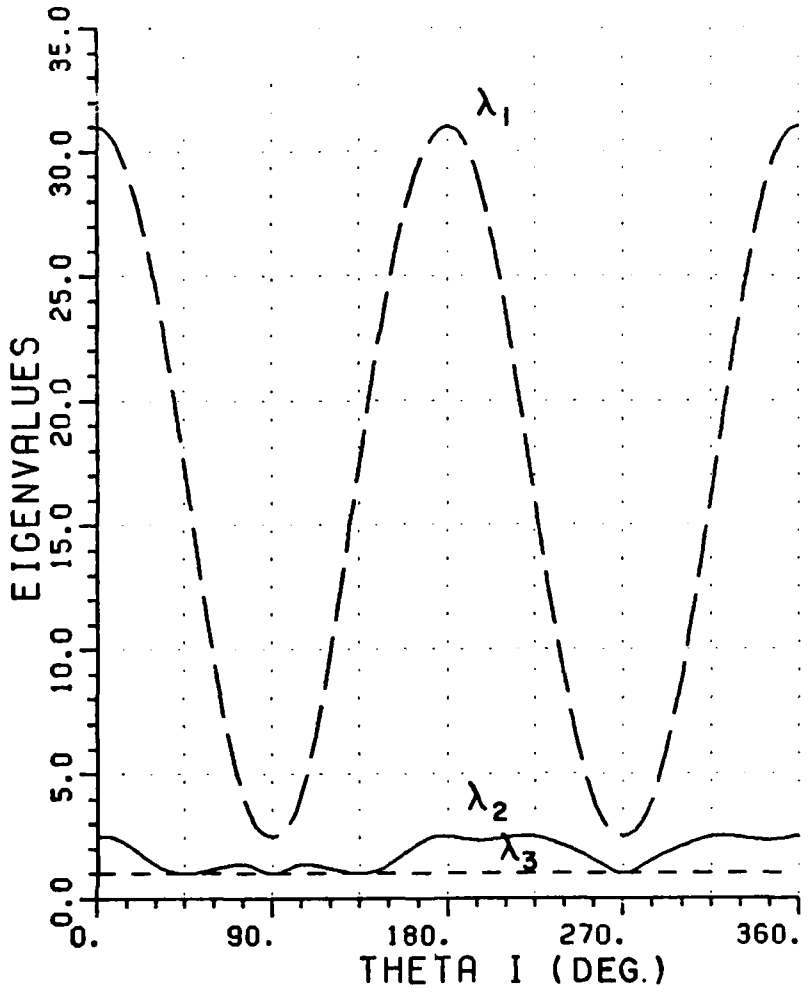

Figure 19. Eigenvalues vs. θ_i for dipole (cosine) elements.

SRI=1.0
INR=10.
BD=0.0
BI=0.0
THETA D=45 DEGREES
3-ELEMENT ARRAY WITH HALF-WAVELENGTH SPACINGS.

From Equation (98), we know that for isotropic elements, $\lambda_{1_{min}}$ occurs when the two signal vectors are orthogonal, i.e., when

$$U_i^T U_d^* = 0.$$

It is evident that this condition is satisfied for θ_i=90° or θ_i=270° with cosine elements (although we might not describe this relation as orthogonality).

Considering next the second eigenvalue, we see that λ_2 has additional minima around θ_i=90° and 270°. These minima occur whenever the array behaves as if only one signal is present. We have from Figure 19 that

$$\lambda_{2_{max}} = \frac{5}{2} \quad , \quad \lambda_{2_{min}} = 1 \quad .$$

Theoretically, from Equation (60) and (62) we know that when

$U_i^T U_d^* = 0$ λ_2 will reach its maximum $1+\xi_d U_d^T U_d^*$, which is $\frac{5}{2}$ for θ_d=45°.

Note that the smallest eigenvalue, λ_3, remains at unity. This eigenvalue is not affected by the change in element patterns.

The previous example shows λ_1, λ_2 and λ_3 for cosine elements with weak interference (θ_i=10). We now show how λ_1 and λ_2 behave for cosine elements with strong interference. Suppose we now set ξ_i=1000 with other parameters the same as in Figure 19. We first show λ_1 in Figure 20. From the figure, we see that with cosine elements λ_1 has a range of variation far larger than that for isotropic elements. Because of the pattern nulls around θ_i=90° and 270°, λ_1 varies between a high value of approximately 3×10^3 to a low of 2.5. Thus, λ_1 is very

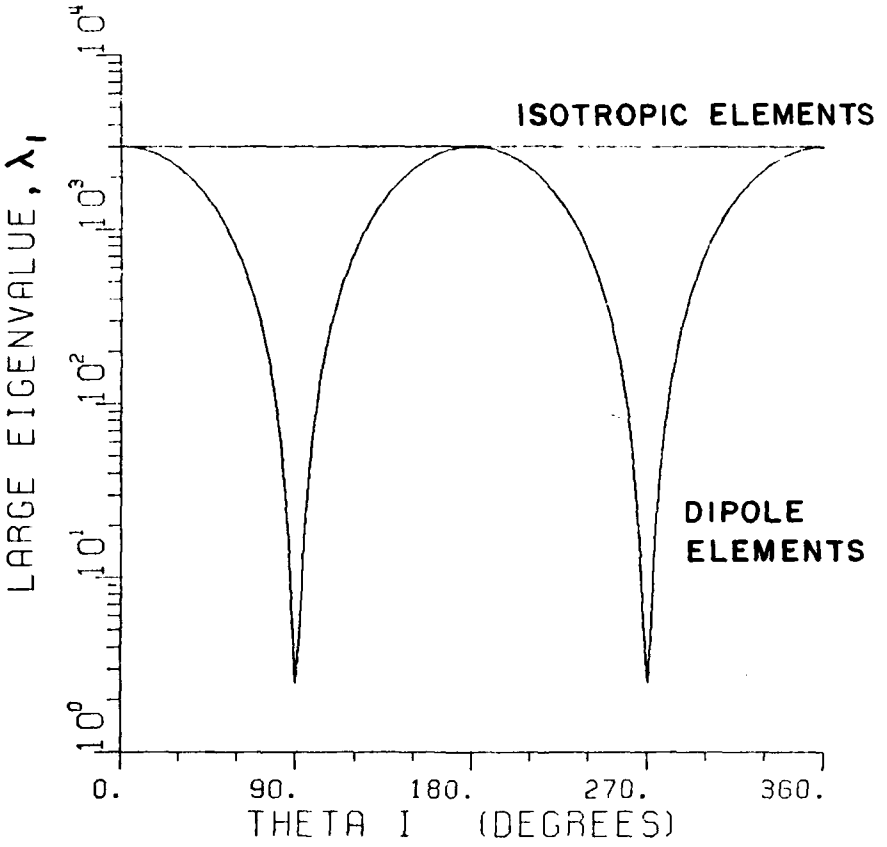

Figure 20. λ_l vs θ_i for isotropic elements and dipole (cosine) elements.
SNR=1
INR=1000
BD=0
BI=0
θ_d=45°
3-ELEMENT ARRAY WITH HALF-WAVELENGTH SPACING.

sensitive to the element patterns and, of course, can no longer be viewed as a constant.

Figure 21 shows λ_2 for both isotropic and cosine pattern elements. In general, λ_2 has the same shape for both cases except around the pattern nulls at θ_i=90° and 270°. Within the region around these pattern nulls (indicated by A and A'), the interference is nulled by the element patterns. I.e., the array behaves as if only one (the desired) signal is present.

Notice that around these null regions (A and A'), λ_2-1 is not related to the output SINR because the condition $\xi_i U_i^T U_i^* \gg \xi_d U_d^T U_d^*$ is not met.

Next, consider what happens if the element patterns are rotated so the elements have beam maxima and nulls in different directions. Rotating the elements eliminates the symmetry null at $\theta_i=180°-\theta_d$. For example, in the element patterns $f_\ell(\theta)=\cos(\theta+\delta_\ell)$, let us set

$$\delta_1=-60°, \quad \delta_2=0° \quad \text{and} \quad \delta_3=60°.$$

λ_1 for this situation is shown in Figure 22. Notice that the range of variation is smaller than that for the unrotated pattern case. We have from the figure

$$\lambda_{1_{max}} = 1502.5 \text{ and } \lambda_{1_{min}} = 1501.$$

$\lambda_{1_{min}}$ does not drop to a low value because when the interference is nulled by one element, it can still be picked up by the other two elements since the elements have different null directions. λ_1 is essentially constant in this case.

In Figure 23, we show λ_2 for the rotated elements. Notice that the only angle where λ_2 reaches its minimum is $\theta_i=\theta_d=45°$. For all

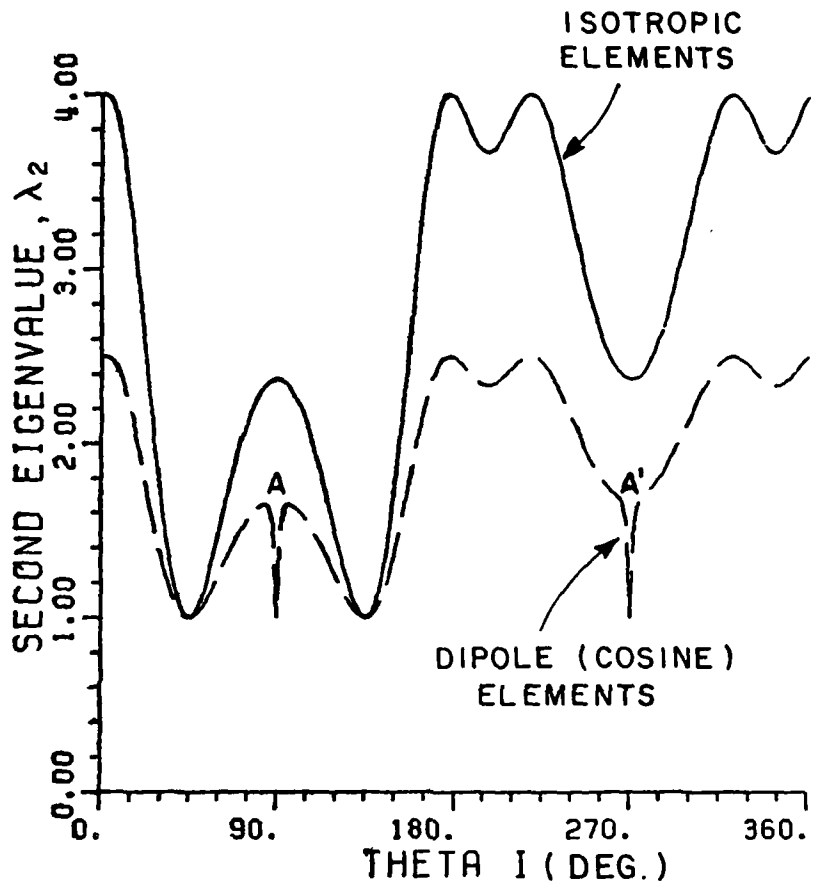

Figure 21. Effect of element patterns.

SNR=1.0
INR=1000
BD=0.0
BI=0.0
THETA D=45 DEGREES
3-ELEMENT ARRAY WITH
HALF-WAVELENGTH SPACINGS.

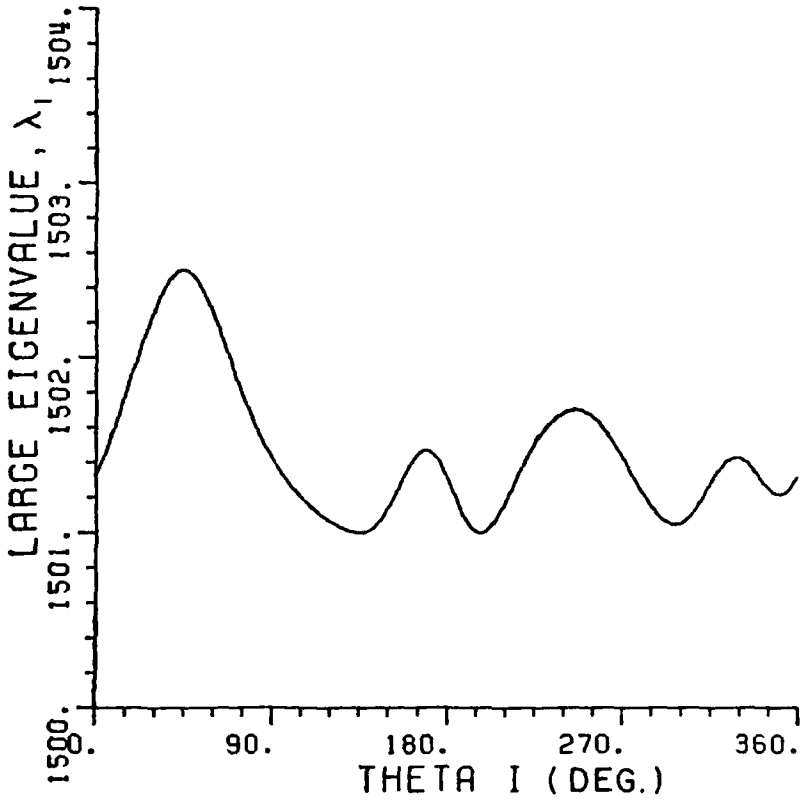

Figure 22. λ_1 vs. θ_i with rotated elements.

SNR=1
INR=1000
BD=0.0
BI=0.0
θ_d=45°
3-ELEMENT ARRAY WITH HALF-WAVELENGTH SPACINGS AND ROTATED COSINE PATTERNS.

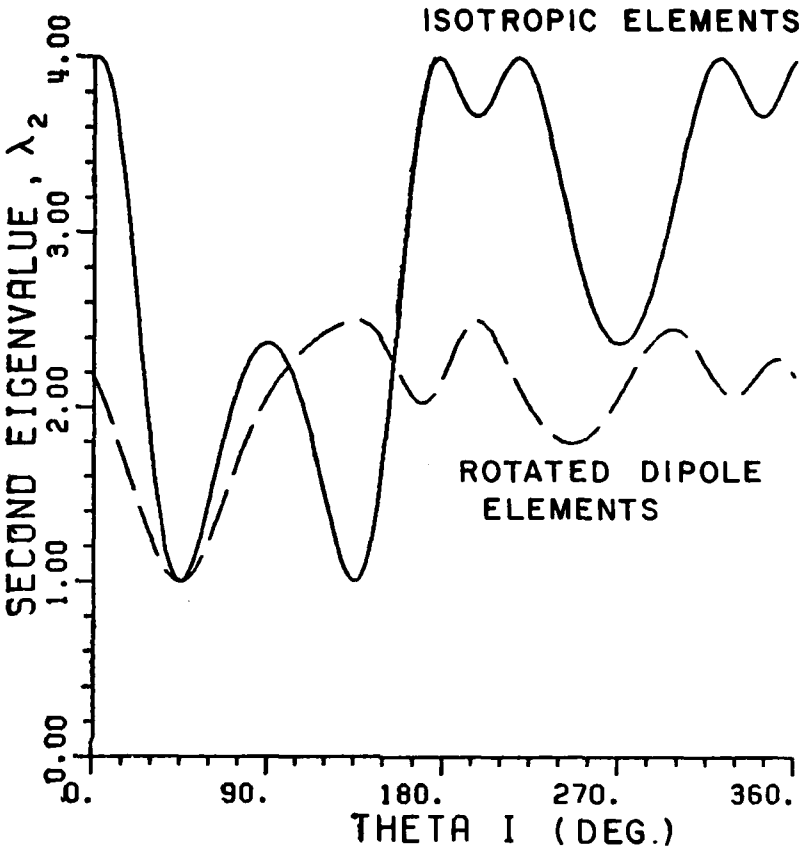

Figure 23. λ_2 vs. θ_i with rotated elements.

SINR=1., INR=1000.
BD=0.000, BI=0.000,
THETA D=45. DEGREES
3-ELEMENT ARRAY WITH HALF-
WAVELENGTH SPACING
COSINE PATTERNS WITH TITLE=60°.

other values of θ_i we have $\lambda_2>1$. From Equation (152), we know that the array output SINR has only one substantial dip at $\theta_i=\theta_d$. The corresponding dip due to symmetry at $\theta_i=180°-\theta_d$ has been eliminated by the rotation of the elements.

Because λ_3 is independent of the element patterns, we know that the smallest eigenvalue remains at unity.

E. The Effect of Signal Bandwidth

The previous sections have discussed the eigenvalues for CW signals. We shall now study the effect of signal bandwidth on the eigenvalues.

In Equation (43), the ℓm^{th} element of the covariance matrix Φ was given for the non-zero bandwidth case. We first normalize this equation with respect to the noise power σ^2, i.e.,

$$\Phi'_{\ell m} = f^*_\ell(\theta_d) f_m(\theta_d) \xi_d \operatorname{sinc}\left[\frac{1}{2} B_d(\phi_{d_\ell} - \phi_{d_m})\right] e^{j(\phi_{d_\ell} - \phi_{d_m})}$$
$$+ f^*_\ell(\theta_i) f_m(\theta_i) \xi_i \operatorname{sinc}\left[\frac{1}{2} B_i(\phi_{i_\ell} - \phi_{i_m})\right] e^{j(\phi_{i_\ell} - \phi_{i_m})}$$
$$+ \delta_{\ell m} \quad .$$

From these matrix elements, we have obtained the normalized eigenvalues of Φ' by a subroutine in the IBM Scientific Subroutine Package [9]. The subroutine is based on the Jacobi method (modified by Von Neumann[10,11]). We shall first show the effect of desired signal bandwidth on the eigenvalues and then the effect of interference bandwidth. We consider again an array with three isotropic elements a half wavelength apart. The signal-to-noise ratios are assumed to be ξ_d=1 and ξ_i=1000 with θ_d=45°.

We first show how λ_2 varies for different desired signal bandwidths, B_d, in Figure 24. B_d has been increased from zero to one in steps of 0.2 and B_i is kept at zero. In the sector $25° < \theta_i < 155°$, we see that λ_2 increases with increased B_d, so the time constant of the array associated with λ_2 becomes smaller. On the other hand, for interference coming from outside that sector, λ_2 decreases with increased B_d and the associated time constant is larger. The combined effect of the above two results is that the range of variation of λ_2 is reduced with increased B_d. For example, with B_d 0.4, we have

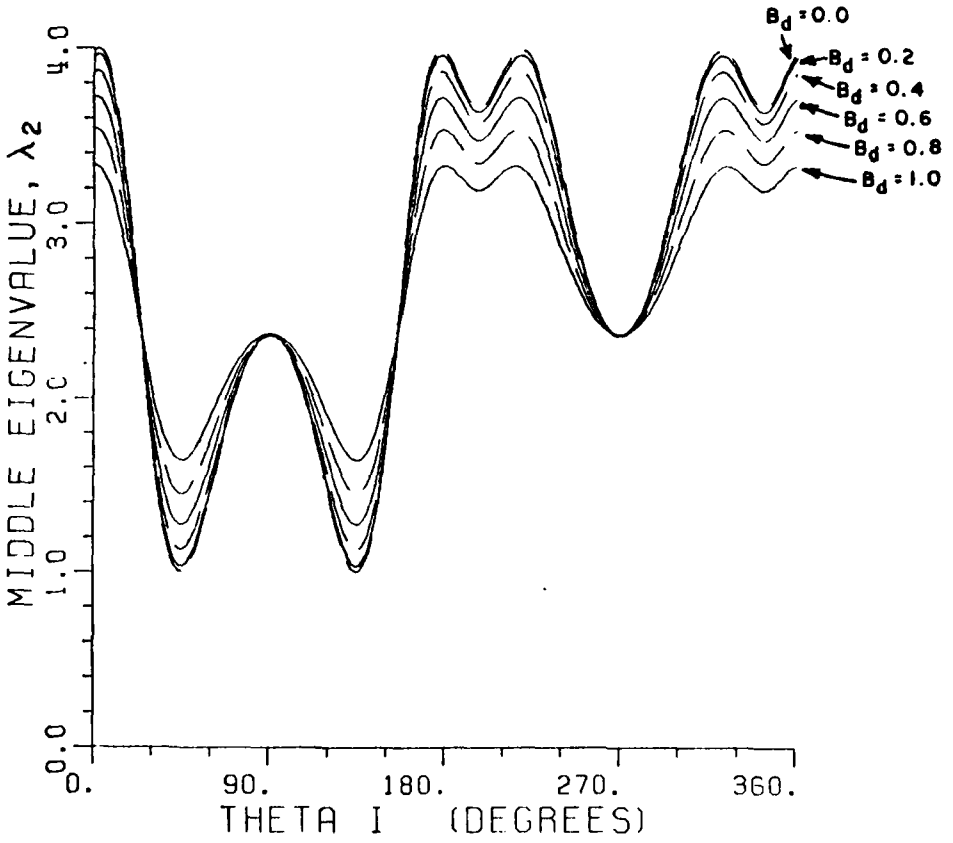

Figure 24. Effect of B_d on λ_2.

SNR=1
INR=1000
θ_d=45°
B_i=0
B_d is changed.

$$\lambda_{2_{max}} \doteq 3.88 \text{ and } \lambda_{2_{min}} \doteq 1.12$$

so the range of λ_2 has been reduced to 2.76 (an 8% change from 3) with 40% change in the desired signal bandwidth. Notice that $\lambda_{2_{min}}$ is no longer unity for non-zero B_d.

We now consider λ_3. With non-zero bandwidth, λ_3 is no longer constant. In Figure 25, we show how λ_3 increases with increased B_d. With B_d=0.4, we find

$$\lambda_{3_{max}} \doteq 1.15 \qquad \lambda_{3_{min}} \doteq 1.05 \quad .$$

The time constant associated with λ_3 decreases with increased B_d.

Because the sum of the three eigenvalues is a constant, we can obtain the behavior of λ_1 with B_d from Figures 24 and 25. However, since the changes in both λ_2 and λ_3 (hence in λ_1) are very small (.5 for B_d=1) compared to the magnitude of λ_1, which is around 3000, it turns out that λ_1 is still essentially constant for B_d=1.

Now let us discuss the effect of interference bandwidth, B_i. In Figure 26, we have calculated λ_2 for various B_i. It is seen that λ_2 is more sensitive to B_i than to B_d because a small (5%) increase in B_i causes λ_2 to increase significantly while a large (40%) increase in B_d makes λ_2 change only slightly (8%). This difference is due to the fact that the interference is very much stronger than the desired signal.

From the figure, we see that λ_2 increases with B_i. Also, notice that when the interference is coming from broadside (θ_i=0° or 180°), λ_2 has a low value. This phenomenon occurs because for these arrival angles there is no interelement delay for the interference so the interference has the same effect on the covariance matrix as a CW

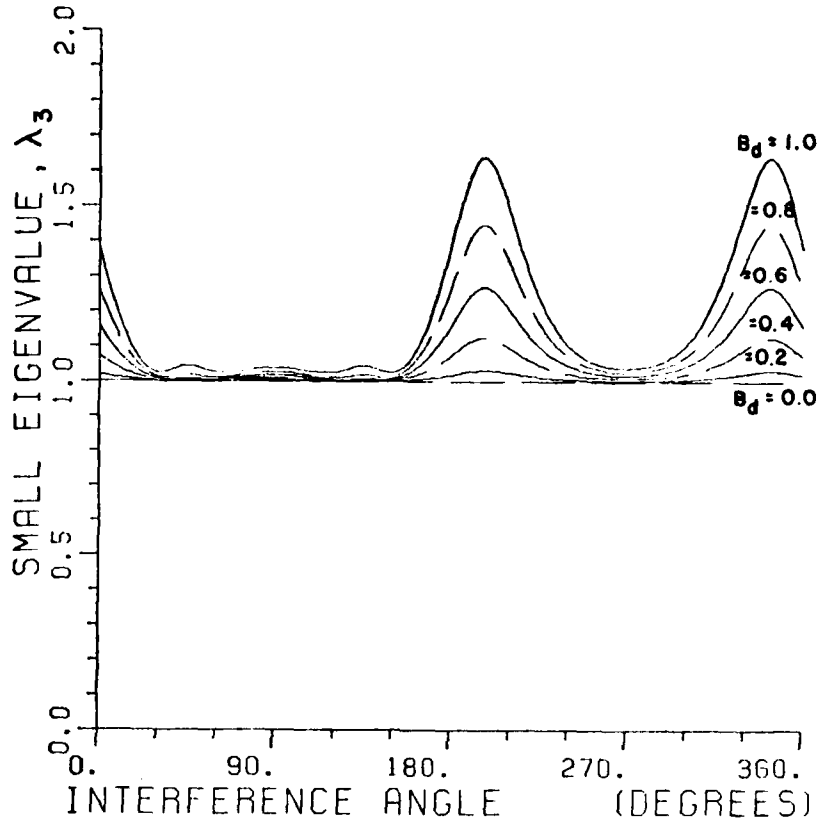

Figure 25. Effect of B_d on λ_3.
SNR=1.
INR=1000.
THETA D=45.
BI=0.00
BD is changed.

signal. From the previous result in Equation (90) we know that λ_2 is bounded by $1+\varepsilon_d U_d^T U_d^*$ for CW signals, so λ_2 is approximately 4 at θ_i=0° and 180°, as shown

The effect of B_i on the small eigenvalue, λ_3, is shown in Figure 27. As B_i increases, λ_3 also increases and exhibits more complicated behavior.

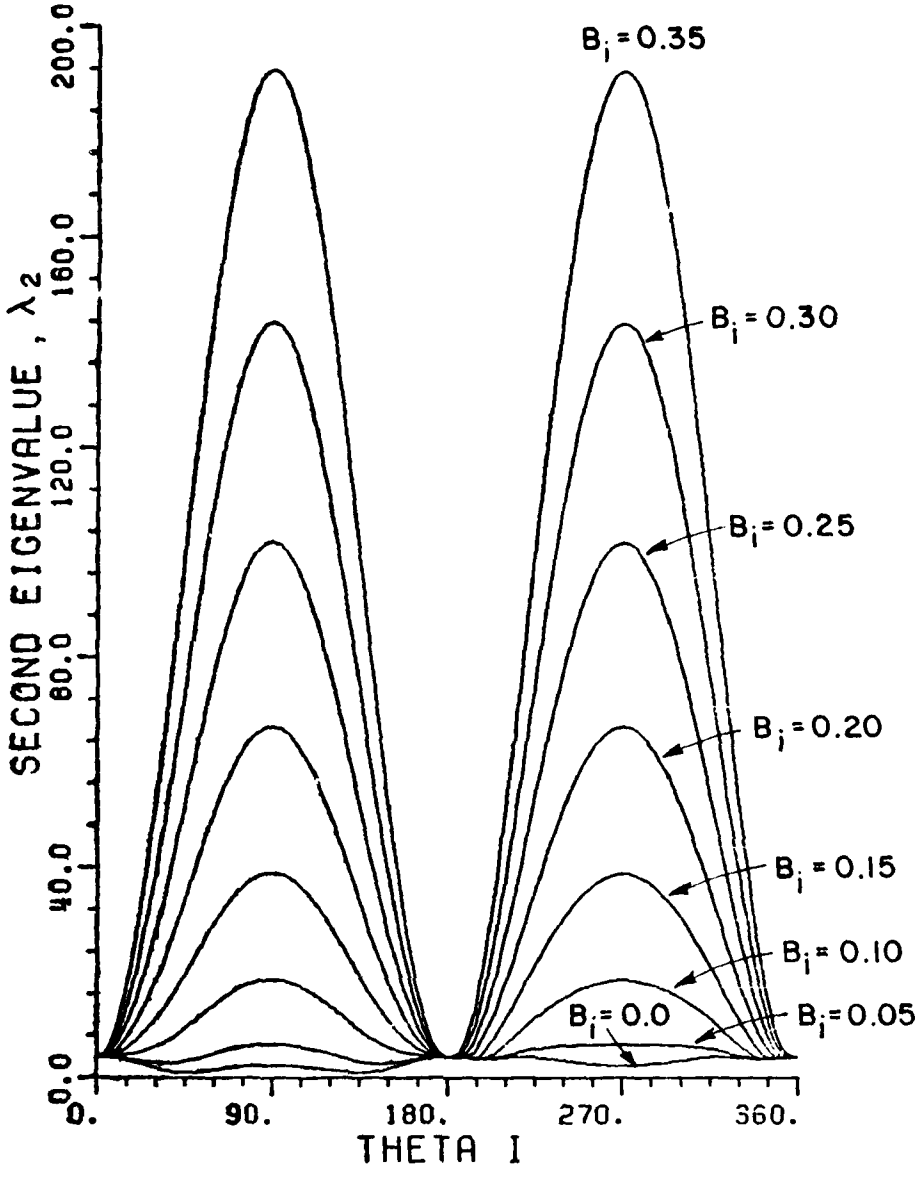

Figure 26. Effect of β_i on λ_2.

SNR=1
INR=1000
β_d=0
θ_d=45°
β_i is varied.

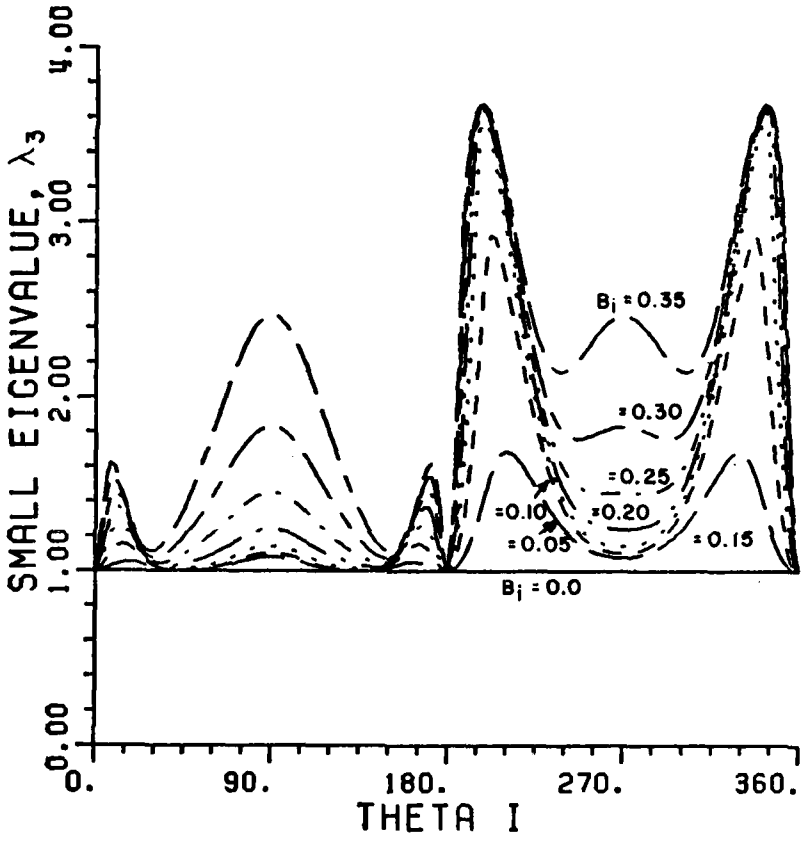

Figure 27. Effect of B_i On λ_3.

SNR=1.
INR=1000.
BD=0.00
THETA D=45.0

Since λ_2 and λ_3 increase with B_i and the sum of the three eigenvalues is a constant, we conclude that λ_1 must decrease with increased B_i. However, the percentage change in λ_1 caused by B_i is still small because λ_1 is large. For example, with B_i=0.2, we see from Figures 24 and 25 at θ_i=90°

$$\lambda_2 = 66 \quad , \quad \lambda_3 = 1.2,$$

so from $\lambda_1+\lambda_2+\lambda_3 = 3006$ we know

$$\lambda_1 = 2938.8.$$

Thus λ_1 decreases from its value of 3002.6 for CW to 2938.8 with 20 percent interference bandwidth. The percentage change is less than 2 percent, i.e.,

$$\frac{3002.6-2938.6}{3002.6} < 2\% \quad .$$

Therefore, the effect of B_i on λ_1 is rather small.

In conclusion, increased interference bandwidth causes λ_2 and λ_3 to increase and λ_1 to decrease. The time constants associated with λ_2 and λ_3 will decrease with B_i and that associated with λ_1 will increase. Desired signal bandwidth causes the range of variation of λ_2 to decrease and that of λ_3 to increase. In addition, λ_1 is little affected by both B_d and B_i provided that $B_d \leq 1$ and $B_i \leq 0.2$.

CHAPTER IV
CONCLUSIONS

In this report, we have first derived the eigenvalues of the covariance matrix for an N element adaptive array with a CW desired signal and a CW interference. There are N-2 constant eigenvalues in this case. The remaining two eigenvalues depend on the signal environment and have been shown to vary within certain bounds. Hence the eigenvalue spread, defined as the ratio between the two eigenvalues, is also bounded, as in Equation (110).

Furthermore, we have discussed the effects of various signal and array parameters on the eigenvalues. It has been shown that when the interference is strong, the largest eigenvalue is essentially constant for isotropic elements. This large eigenvalue exhibits little percentage change as the signal angles are varied. The large eigenvalue remains constant regardless of element spacing or signal bandwidth. It does depend on the input INR, the number of elements and the element patterns, however.

We have also shown that the second eigenvalue, λ_2, approaches a limit when ξ_i is increased. For large ξ_i and CW signals, the array output SINR is one less than this limit, as shown in Equation (152). The higher ξ_i the better the approximation. As the input SNR, ξ_d, is increased, the range of variation of λ_2 becomes larger. λ_2 is very sensitive to element spacings and element patterns. By manipulating element spacings and patterns, we can modify the behavior of λ_2 and also the array output SINR. In addition, λ_2 depends very much on B_i; a small increase in B_i causes λ_2 to increase significantly, as demonstrated in Figure 26. In the case of greatest interest where ξ_d is

much lower than ξ_i, the effect of desired signal bandwidth on λ_2 is much less.

The remaining N-2 eigenvalues will differ from unity only when non-zero bandwidth signals are present. Also, the effect of B_i on λ_3 is larger than that of B_d when the interference is much stronger than the desired signal.

REFERENCES

1. S.P. Applebaum, "Adaptive Array," Trans. IEEE, AP-24, 5 (September 1976), 585.

2. B. Widrow, P.E. Mantey, L.J. Griffiths and B.B. Goode, "Adaptive Antenna Systems," Proc. IEEE, 55, 12 (December 1967), 2143.

3. W.F. Gabriel, "Adaptive Arrays - An Introduction," Proc. IEEE, 64, 2 (February 1976), 239.

4. J.T. Mayhan, "Adaptive Nulling with Multiple-Beam Antennas," Trans. IEEE, AP-26, 2 (March 1978), 267.

5. J.T. Mayhan, "Bandwidth Characteristics of Adaptive Nulling Systems," Trans. IEEE, AP-27, 3 (May 1979), 263.

6. A. Ishide and R.T. Compton, Jr., "On Grating Nulls on Adaptive Arrays," Trans. IEEE, AP-28, 4 (July 1980), 467.

7. A.S. Householder, The Theory of Matrices in Numerical Analysis, Dover Publications, Inc., New York, (1964), 3.

8. R. Bellman, Introduction to Matrix Analysis, McGraw-Hill Book Co., New York, (1970), Second Edition, 64.

9. System/360 Scientific Subroutine Package, Version III, p. 164, EIGEN, International Business Machines Corp., New York, (1970).

10. A.S. Householder, op. cit., Chapter 7.

11. D.M. Young and R.T. Gregory, A Survey of Numerical Mathematics, Addison-Wesley Publishing Co., Reading, Mass., (1973), Chapter 14.